



Aquaporin (AQP) gene family in Buffalo and Goat: Molecular characterization and their expression analysis



Shiveeli Rajput^a, Devika Gautam^a, Ashutosh Vats^a, Mayank Roshan^a, Priyanka Goyal^b, Chanchal Rana^a, Payal S.M.^b, Ashutosh Ludri^c, Sachinandan De^{a,*}

^a ICAR-National Dairy Research Institute (NDRI), Animal Biotechnology Division, Animal Genomics Lab, Karnal 132001, Haryana, India

^b Animal Biochemistry Division, ICAR-National Dairy Research Institute (NDRI), Karnal 132001, Haryana, India

^c Department of Physiology, ICAR-National Dairy Research Institute (NDRI), Karnal 132001, Haryana, India

ARTICLE INFO

Keywords:

Aquaporins (AQPs)
Aquaglyceroporins (AQGPs)
Membrane intrinsic proteins (MIPs)
Cloning
Tissue specific gene expression

ABSTRACT

Aquaporins (AQPs) are essential membrane proteins facilitating water and small solute transport across cell membranes. Mammals have approximately 13 paralogs of AQPs that may have evolved through gene duplication events. These genes are present in two separate clusters within the genome. In the present study, comprehensive 13 AQP genes (*AQPO–12*) were cloned and characterized in buffalo and goat. The protein coding region of AQPs in both species ranged from 729 to 990 bps, corresponding to 263–330 amino acid residues. Two important residues including NPA motifs and ar/R selectivity filter were found conserved in all AQPs, except for *AQP7*, 11 and 12. *AQPO*, 2, 4, 5, 7, 9, 12 showed tissue-restricted expression, whereas *AQP1*, 3, 8, and 11 exhibited ubiquitous expression across several tissues. *AQP10* was identified as a pseudogene in all artiodactyls. Transcript variants were identified in buffalo and goat, where some variants of goat *AQP5* and 6 lacked important motifs. Evolutionary analysis indicated positive selection at or near the NPA motifs and ar/R selectivity filter of *AQPO*, 3, 6, 7, and 10 that may alter its structure and function. This study is crucial for future investigations aiming to study the molecular mechanisms of AQPs in response to various physiological conditions.

1. Introduction

Aquaporins (AQPs), also known as Major Intrinsic Proteins (MIPs), are essential membrane proteins that act as channels for the passage of water and occasionally, tiny solutes. All organisms including micro-organisms and higher eukaryotes such as animals, and plants have preserved AQPs, performing the same function [1,2]. AQPs have six transmembrane helices that are structured as monomers, dimers, and tetramers to produce pores in the plasma membrane. The six transmembrane-helices connected by five connecting loops (loops A–E), and the cytoplasmic N- and C-termini forms an independent pore that controls the transport activity [3].

Two highly conserved Asparagine-Proline-Alanine (NPA) motifs and an aromatic/arginine (ar/R) selectivity filter are crucial for the function of these channels. The NPA motifs located in loops B and E are responsible for the pore formation, whereas the ar/R region made up of four residues from helix H2 and H5, loop E1 and E2 regulates the substrate selectivity, hydrophobicity, and pore width [4–6]. Variations in

the amino acid residues of NPA motifs and ar/R selectivity filter are believed to alter the substrate specificity [7]. The divergence between the orthodox Classical AQPs and Aquaglyceroporins (AQGPs) occurred early in the cellular evolution [8,9]. Based on the permeation specificities, AQPs are classified into four major groups: (i) Water selective classical AQPs (*AQPO*, *AQP1*, *AQP2*, *AQP4*, *AQP5*, *AQP6*); (ii) Aquaglyceroporins (*AQP3*, *AQP7*, *AQP9*, and *AQP10*) that are permeable to glycerol, urea, water, and other small solutes; (iii) Unorthodox AQPs (*AQP11* and *AQP12*); (iv) *AQP8* type aqua-ammoniaporins (*AQP8*) [8,10,11]. Whole genome duplications (WGD) and tandem duplications (TD) are the key drivers of eukaryotic evolution, producing multiple AQP paralogs. Rapeseed and Upland cotton have the largest repertoires, with up to 120 and 71 paralogs, respectively, whereas mammals have 17 paralogs due to tandem duplication of *AQP7* and *AQP12* [12,13]. Some duplicated genes tend to have redundant functions, such as *AQP7* and *AQP10* is a pseudogene in rodents [14].

Mammalian AQPs are essential for several physiological and pathophysiological processes, such as organogenesis, osmoregulation,

* Corresponding author at: AGL, Animal Biotechnology Division, ICAR-National Dairy Research Institute, Karnal, HR, India.

E-mail address: sachinandan@gmail.com (S. De).

regeneration, lipid metabolism, tumour angiogenesis, renal water absorption, fat metabolism, reproduction, and liver gluconeogenesis [15–18]. These membrane proteins are widely distributed, particularly in cells involved in fluid transport such as epithelial cells in different organs [3]. AQP0 exhibits widespread expression in the lens fiber cells of the eye in human and mice, crucial for maintaining water homeostasis and lens transparency [19,20]. AQP1 and 3, widely expressed in the body, play pivotal role in regulating cell growth, migration, angiogenesis, skin epidermis, hydration, and proliferation of keratinocytes in human, rat, and mice [3,21,22]. AQP2 and 6, predominantly expressed in the apical region of renal collecting duct are regulated by antidiuretic hormone arginine vasopressin (AVP). Binding of AVP to vasopressin V2 receptor (V2R) prompts the translocation of AQP2 to the apical membrane of kidney, facilitating water reabsorption from the pro-urine and consequent urine concentration in human, mice, and birds [23–26]. AQP4, predominantly expressed in central nervous system (CNS) in human, plays a vital role in neuroexcitation, and astrocyte migration following injury [27]. Similarly, AQP5, present in secretory glands and alveolar epithelium, facilitates the generation of saliva, tears, and pulmonary secretions in humans and mice [25,28]. AQP7 is abundantly expressed in testis, adipose tissue, and nephrons of the kidney in human and mice, facilitating the transport of glycerol, water, urea, ammonia, and arsenite [23,29]. AQP8 is implicated in transporting hydrogen peroxide (H_2O_2) across mitochondrial membranes in situations when reactive oxygen species (ROS) is generated [21,25]. AQP9, highly expressed in the testis, liver, brain, and leukocytes in human and mice, plays a crucial role in metalloid homeostasis by transporting arsenite and antimonite [8,30]. AQP10, along with AQP7, maintain the normal glycerol levels in adipocytes, although it is a pseudogene in mice and bovines [31,32]. AQP11 and 12 are the unorthodox class of AQPs that are expressed in tissues like kidney, liver, testis, ovary, pancreas, and duodenum [25].

AQPs have been widely distributed and studied in plants [33], unicellular organisms [34], invertebrates [35] and vertebrates [36]. However, limited information is available about the sequencing and tissue-wide distribution of the aquaporin gene family in mammals, particularly ruminants. Ruminants such as buffalo and goats play a major role in agricultural economy through milk, meat, and mechanical power. Since the aquaporin sequence, gene structure, secondary structure, motif structure, evolutionary relationships and expression patterns have not been fully characterized in ruminant species, thus current efforts are directed towards the characterization and expression analysis of aquaporin gene family in ruminants.

2. Materials and methods

2.1. Ethical statement

Ethical approval was not required from the Institutional Animal Ethics Committee (IAEC) of ICAR-National Dairy Research Institute, Karnal, Haryana as buffalo and goat tissue samples were collected from municipal slaughterhouse (Gazipur, New Delhi and Karnal, Haryana). The experiment was approved IAEC no. 42-IAEC-18-6, as per the article no. 13 of the CPSEA rules, Government of India, for collecting blood samples from buffalo.

2.2. Sample collection

A total of 15 buffalo tissues (brain, bone marrow, eye lens, heart, liver, lymph node, ovary, pancreas, rumen, small intestine, spleen, testis, tongue, and tonsils) and 11 goat tissues (eye lens, heart, kidney, liver, ovary, rumen, spleen, small intestine, testis, tongue, and tonsils) from six different animals were collected in RNA later and used for RNA isolation. To isolate peripheral blood cells (PBMCs), monocytes, and WBCs, blood (4 ml) was collected from buffalo (*Bubalus bubalis*) and immediately processed for maintaining the viability of cells. PBMC's

from buffy coat were isolated by density gradient centrifugation at $300 \times g$ using HiSepTM LSM 1077 (HiMedia, India). Monocytes were isolated using the plastic adherence method and carefully collected in Tri-reagent (T9424, Sigma Aldrich, Merck, Germany) after 2 h [37]. Buffalo fibroblast cells were cultured and maintained in complete Dulbecco's Modified Eagle's medium (DMEM) (Sigma, Aldrich) supplemented with 10 % Fetal Bovine serum (FBS) (Invitrogen), L-Glutamine 2 mM, 25 mM HEPES, 10,000 Uml⁻¹ Penicillin-G and 100 μgml^{-1} streptomycin (Gibco, Thermo Scientific) at 37 °C and 5 % CO₂ [38]. Whole Blood cells (WBCs) were isolated from Blood using 1× RBC lysis buffer.

To isolate Alveolar macrophages A.MΦ, the bronchi and alveoli of buffalo and goat lungs were filled with Hank's Balanced Salt Solution (HBSS) supplemented with 10,000 Uml⁻¹ and 100 μgml^{-1} of Penicillin G/Streptomycin and gently massaged; this process was repeated two–three times. The alveolar lavage solution containing A.MΦ was centrifuged at $200 \times g$ for 5 min at 4 °C and the resulting cells washed with PBS were then placed in a 100 mm NunclonTM Delta surface tissue culture dish [39]. The adhered cells were harvested using Tri-reagent.

2.3. Total RNA, DNA extraction and complementary DNA (cDNA synthesis)

Total RNA was isolated from buffalo and goat tissues/cells as mentioned above, using Tri-reagent, as per manufacturer's instructions. The quality and quantity of RNA samples were checked on 2 % agarose gel electrophoresis and were further ascertained using Nanodrop2000 spectrophotometer (Thermo Scientific, USA). 5 μg of each RNA sample was reverse transcribed into cDNA using the RevertAid First Strand cDNA synthesis kit (K1622, Thermo Fisher scientific). Genomic DNA was isolated from blood of the ruminants (buffalo, cattle, goat, and sheep) using a standard phenol chloroform extraction method [40].

2.4. PCR amplification, cloning and sequencing of aquaporin genes

The oligonucleotide primers for the full-length coding regions of AQP genes (AQP0–12) (Table S2) were designed from the conserved regions of the predicted sequences of ruminants from National Center for Biotechnology Information (NCBI) (<https://www.ncbi.nlm.nih.gov/>) and were further verified by analyzing at UCSC genome browser. The complete coding regions of buffalo and goat AQP genes were amplified from different tissues and cells (eye lens, kidney, spleen, lungs, fibroblast, A.MΦ, testis and liver). AQP10 gene was amplified from the genomic DNA of ruminants (buffalo, cattle, goat, and sheep). The amplification conditions are included in Table S3. The amplified PCR fragments of all genes were purified using NucleoSpin gel extraction kit as per manufacturer's instructions. The purified product of each AQP gene was cloned using CloneJet PCR cloning kit (K1232, Thermo scientific) and transformed into XL1-Blue competent cells using 50 mg/ml ampicillin as a selection marker. The positive recombinant clones were screened and sequenced through capillary sequencing by sanger dideoxy method.

2.5. Data acquisition

We retrieved a total of 248 coding mRNA and protein sequences of AQPs from the non-redundant nucleotide and protein database (nr) maintained by NCBI with an e-value of $1e^{-15}$ as a cutoff, through BLASTN and BLASTP (nucleotide-nucleotide and protein-protein BLAST). For our analysis, we examined the retrieved sequences of 20 vertebrate species from different orders, including Artiodactyla (buffalo, cattle, goat, oryx, whale, sheep, elk, camel, pig); Perrisodactyla (rhinoceros, horse); Chiroptera (bat); Carnivora (Dog); Diprotodontia (brushtail possum); Monotremata (echidna); Crocodilia (alligator); Anura (frog); Galliformes (jungle fowl). The detailed sequence information is included in the Tables S8–10. The physicochemical properties including the molecular weight, isoelectric pI was calculated using

Protparam tool (<https://web.expasy.org/protparam/>). The conserved MIP domain of the AQPs were determined using conserved domain search server (CDD) of NCBI [41] and Simple Modular Architecture Research Tool (SMART) [42]. The protein sequences encoding the MIP domain of AQPs was aligned using the MUSCLE program of MEGAX software [43].

2.6. Evolutionary analysis of AQPs

To determine the evolutionary relationship among the AQPs, the maximum likelihood (ML) analysis was performed through Randomized Axelerated Maximum likelihood (RAxML) program version 8.2.10 [44]. The ML based phylogenetic tree was reconstructed using the GTR (general time reversible)+GAMMA protein substitution model and the reliability of each branch was determined using the 1000 standard non-parametric bootstrap replications [45]. The ML tree was further used for site-specific and branch-site selection pressure studies. The gene duplications were determined using the gene duplication wizard under MEGAX software [43].

2.7. Selection pressure analysis

In order to detect positive selection in artiodactyla and other vertebrate lineages, we performed the branch-site test (null model MA vs. model MA) [46,47]. The branch-site models allows the reliable detection of positive selection sites with low false positive rates, on one or more selected branches (foreground branches) in contrast to the background branches [48]. The ML phylogenetic tree and multiple sequence alignment (MSA) using the coding sequences of AQPs were analysed using the Bayes Empirical approach in the CODEML program of the PAML v.4.9 software and the EasyCODEML package [49–51]. We calculated the LRTS of both null model MA (null hypothesis) and model MA (alternate hypothesis), using a χ^2 test at a *P* value of 0.05, to determine the statistically significant model. We conducted several branch-site tests for each aquaporin gene, selecting different lineages (foreground branches) in each case. Since several tests were conducted, the multiple test correction of the LRT *p* values was performed to calculate the corrected *p* values (Q-values) for a false discovery rate (FDR) [52] using the Microsoft Excel software. The lineages (clades) with LRT *p*-value <0.05 were further considered to indicate positive selection.

2.8. Molecular docking study

To explore the binding potential and function of AQPs, molecular docking was performed using AutoDock4 tool. The Autodock4 tool uses the lamarckian genetic algorithm and grid-based method to allow rapid determination of binding energy of trial conformations [53]. The structures of solutes (glycerol, urea); inhibitors (DFP00173, and Z433927330) were retrieved from NCBI Pubchem (<https://pubchem.ncbi.nlm.nih.gov/>) and the three-dimensional models of AQP3 and AQP7 were created using homology-based server, Swiss Modeler (<https://swissmodel.expasy.org/>) and AlphaFold (<https://alphafold.ebi.ac.uk/>). Autodock MGL tools (<http://mgltools.scripps.edu/>) were used to generate a grid box with a size of (x = 40, y = 40, z = 40) and a center of (4.373, 0.742, & -0.256); & (-8.131, 4.199, 7.996) that target the active sites of AQP3 and 7 respectively. Docking results were visualised using the Pymol software [54].

2.9. Tissue distribution of AQPs

Real-time quantitative PCR (qRT-PCR) was used to analyse the tissue wide distribution of AQP genes in different tissues and cells of buffalo and goat. The AQP gene expression was assayed using a Light cycler 480 II Real-time PCR machine (Roche Diagnostics, USA). Each qRT-PCR reaction consisted of 2 μ l cDNA, 5 μ l of 2X SYBR Green PCR Master

Mix (KK4609, KAPA SYBR FAST, Sigma Aldrich), 0.5 μ l each of forward and reverse primers (10 pm/ μ l), and nuclease free water in 10 μ l reaction volume. Two technical replicates were set for each cDNA sample, and six biological replicates were set for tissue samples. A standard melting curve analysis was performed to assess the accuracy of PCR in the form of single qRT-PCR product. Statistical analysis of qRT-PCR data was performed against the Ct values of the ribosomal protein S18 (*RPS18*) housekeeping gene using the $2^{-\Delta\Delta Ct}$ method [55]. The fold changes in the expression were measured relative to *GAPDH* as control of the corresponding candidate gene.

3. Results

3.1. Sequencing and characterization of aquaporins

The full-length sequences of buffalo and goat AQP genes (*AQPO-11*) were identified through RT-PCR from different tissues (Fig. S1). The PCR amplicons of the 11 AQP genes were purified, cloned into blunt end cloning vector (pJET, K1232), and sequenced. The amplified fragments of the AQP genes ranged from 831 to 1110 bps, including the coding region of 630–990 base pairs. Specific genes were amplified from distinct tissues: *AQPO* (884 bp) from the eye lens; *AQP1* and 5 (831–854 bps) from fibroblast cells; *AQP2*, and 6 (853–941 bps) from the kidney; *AQP3* (892 bps) from the spleen; *AQP4* (1110 bps) from the A.M.F; *AQP7*, 8, and 11 (846–1095 bps) from the testis; and *AQP9* (963 bp) from the liver in buffalo and goat (Fig. S1). The obtained AQP gene sequences of buffalo (*n* = 20) and goat (*n* = 24) were submitted to GenBank with accession numbers ON456457-OQ978983 (Tables S4–S5). A homology-based search using BlastN revealed similarities between buffalo and goat *AQPO-11* genes and those of artiodactyla and human, ranging from 99.62 to 83.58 % (Table S6).

The characteristics of the AQP gene family in the genome of buffalo and goat, including the chromosome location, CDS, amino acid length, protein m.wt, pI, GRAVY (Grand average of hydropathy), and subcellular localization are listed in Table S7. The AQP protein molecular weight ranged from 22 to 36 kDa and the pI values ranged from 6.1 to 9.6. Among the AQP proteins, the smallest one was AQP5 with only 210 aa and the largest one was AQP7 with 330 aa long. The subcellular localization indicated that all AQPs were membrane bound and distributed on the plasma membrane (endoplasmic reticulum, golgi, and cytoplasm bound), with potential signal anchor and probable GPI anchor region (Table S7).

3.2. Exon structures, motif distribution and conserved features of AQPs

The exon structures of buffalo and goat AQPs were analysed through comparison with the genomic information available at NCBI and the UCSC genome browser. The analysis revealed that *AQPO*, 1, 2, 5, and 6 in both buffalo and goat consisted of 4 exons while *AQP3* and 8 had 6 exons. *AQP4* and 9 consisted of 7 exons, with *AQP9* of buffalo having 7 exons and that of goat having 6 exons. Additionally, *AQP7* and 11 consisted of 8 and 3 exons in buffalo and goat, respectively.

A total of six motifs were identified in buffalo and goat AQPs, ranging from 20 to 50 amino acids in length (Fig. S2). Based on the InterproScan search, motifs 1, 2, 3, 4, and 5 are involved in the transmembrane transport activity, facilitating water and glycerol transport (Table S1). AQP genes from same type (wAQPs, AQGPs, and unorthodox AQPs) showed similar motif characteristics. In detail, motif 1, 3, 5, and 6 were conserved in all AQPs, while motif 2, 3, and 4 were absent in AQP10 and AQP11 respectively (Fig. S2).

The domain analysis using the NCBI conserved domain database revealed that all AQP genes share a major MIP domain (215–245 bp in length) (Tables S4–S5). The protein sequence alignment of the MIP domain revealed conservation in sequence, NPA motifs at the N and C terminals; and aromatic/arginine (ar/R) selectivity residues. In contrast to AQP0, 1, 2, 3, 4, 5, 6, 8, 9, and 10, other isoforms of AQPs, such as

AQP7, 11, and 12, have non-canonical NPA motifs. AQP7 has asparagine-alanine-alanine (NAA) residues at the N-terminus and a conventional NPA motif at the C-terminus. The AQP11 gene contains N-terminal asparagine-proline-cysteine (NPC) and C-terminal asparagine-proline-threonine (NPT) residues. AQP12 in bovines has NPT residues at the N and C termini (Fig. S3).

3.3. Aquaporin genes have multiple alternatively spliced variants

The obtained nucleotide and protein sequences revealed the presence of transcript variants in *AQP5*, *AQP6*, and *AQP8* gene in buffalo; and *AQP3*, *AQP5*, and *AQP6* in Goat (Fig. 1). The multiple sequence alignment revealed an absence of entire exon2 of 165 bps in the *AQP5* gene, whereas a deletion of 51 bps from exon1 was found in the *AQP6* in Buffalo. In *AQP8*, a deletion of 60 bps was observed from exon4 and exon5 in Buffalo. In goat, we observed loss of 60 bps from exon3 in *AQP3*; and an entire exon3 of 84 bps and 81 bps long was found missing in *AQP5* and *AQP6* respectively (Fig. 1). To verify our results, we performed the BLAT search against the *Bubalus bubalis* and *Capra hircus* genome assembly using the UCSC genome browser and NCBI BLAST search, which confirmed the existence of unique transcript variants in *AQP3*, *AQP5*, *AQP6* and *AQP8* genes (Tables S4–S5). We also identified the existence of transcript variant of *AQP5* in *Bos taurus*, where exon3 was found missing.

3.4. Aquaporin gene paralogs varies in artiodactyla and other vertebrates

The number of *AQP* genes varied across the 20 vertebrate species examined in the present study (Fig. 2). A genome-wide analysis showed that *AQPO*, 1, 2, 3, 4, 5, 8, 9 and 11 genes are present in all species, but

the genomic region of 2.5 kb encoding 4 exons of the *AQP6* is missing in *Alligator sinensis*, *Xenopus laevis* and *Gallus gallus*; and 17.5 kb of *AQP7* is missing in *Alligator sinensis* and *Tachyglossus aculeatus*. Similarly, a genomic region of 2.8 kb encoding 8 exons of the *AQP10* gene is absent in *Tachyglossus aculeatus*, whereas *AQP12* is absent in *Pteropus alecto* (Figs. 2 and 3). The *AQP12* gene is found as a single copy across all species, with *GPR35* and *KIF1A* as flanking genes in certain species. However, in humans, there are two isoforms of *AQP12* known as *AQP12A* and *AQP12B* (Fig. 3).

3.5. *AQP10* is a pseudogene in buffalo and related species

In the present study, *AQP10* was found to be a pseudogene in 8 artiodactyla species including ruminants and some reptiles (Fig. 2). The screening of the genomic database of some orthologous species had insertions and deletions in the exons of the *AQP10* gene. These included *Bubalus bubalis* (buffalo: XM_006044200.3: two bases inserted in one codon and one base substituted in one stop codon of Exon7); *Bos taurus* (cow: XM_024989821.1: two bases inserted in one codon of Exon7); *Capra hircus* (goat: XM_005677552.2: one base inserted in one codon and two bases deleted in one codon of Exon6); *Ovis aries* (sheep: XM_004003657.5: one base inserted in one codon of Exon6); *Cervus canadensis* (elk: XM_043455414.1: one base inserted in one codon; deleted 1 base in one codon of Exon7); *Oryx dammah* (horned oryx: XM_040229914.1: three bases inserted in two codons of Exon5; one base substituted at stop codon of Exon6); *Camelus ferus* (camel: XM_010954085.1: two bases inserted in two codons; one base deleted in one codon and one base substituted at one genomic stop codon of Exon1, 4, 5, and 6); *Delphinapterus leucas* (beluga whale: XM_022559619.2: inserted one base in one codon; deleted one base in one codon;

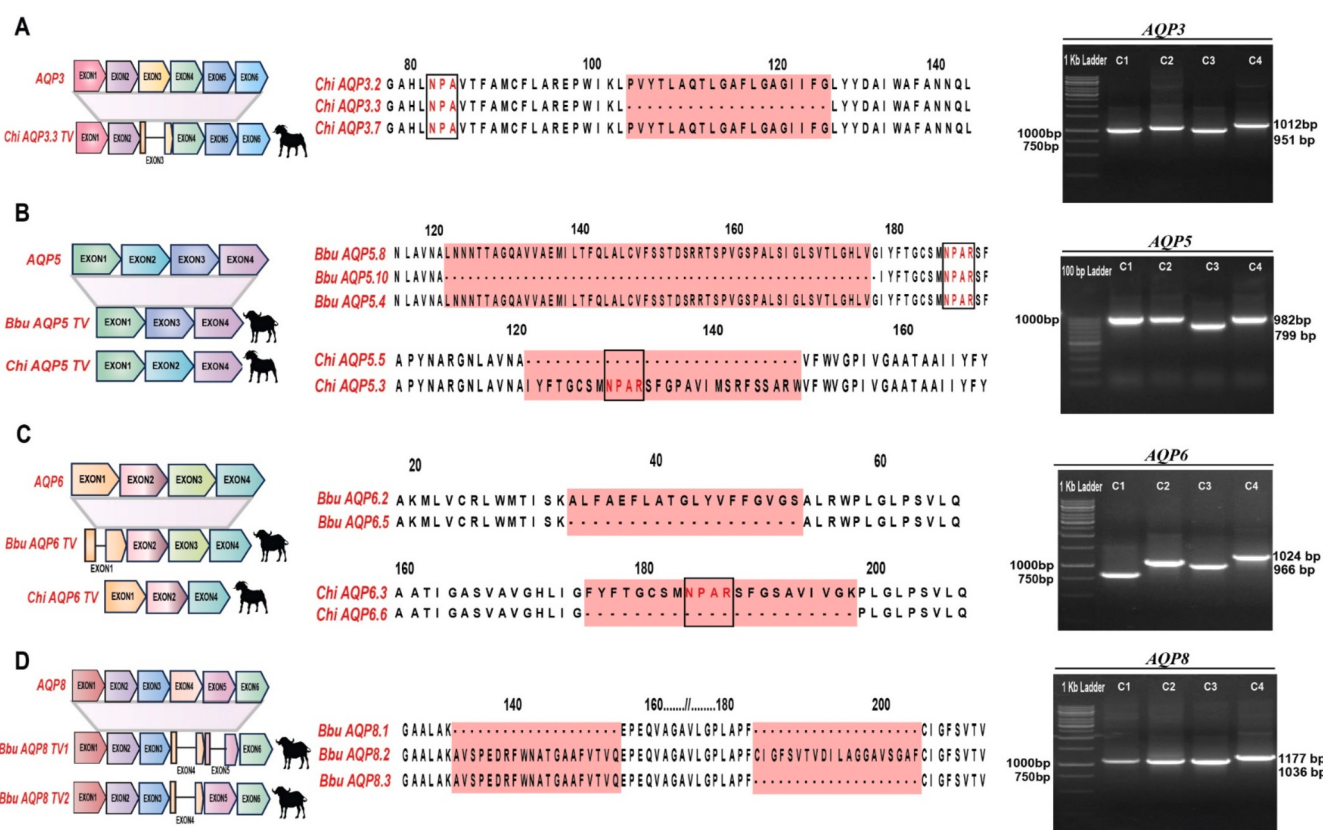


Fig. 1. Comparative analysis of obtained nucleotide and protein sequences of transcript variants in *AQP3*, *AQP5*, *AQP6*, and *AQP8* gene of buffalo and goat. A: Deletion of 60 bps from Exon3 in Goat *AQP3*; B: Whole exon2 (165 bps) and exon3 (60 bps) missing in buffalo and goat *AQP5*; C: Deletion of 51 bps from exon1 and entire exon3 (81 bps) from buffalo and goat *AQP6*; D: In *AQP8*, a deletion of 60 bps was observed from exon4 and 5 in Buffalo. Abbreviations: Bbu: *Bubalus bubalis* (Buffalo); Chi: *Capra hircus* (Goat); AQP: Aquaporins; TV: Transcript variants. Further confirmed by UCSC Genome Brower BLAT search.

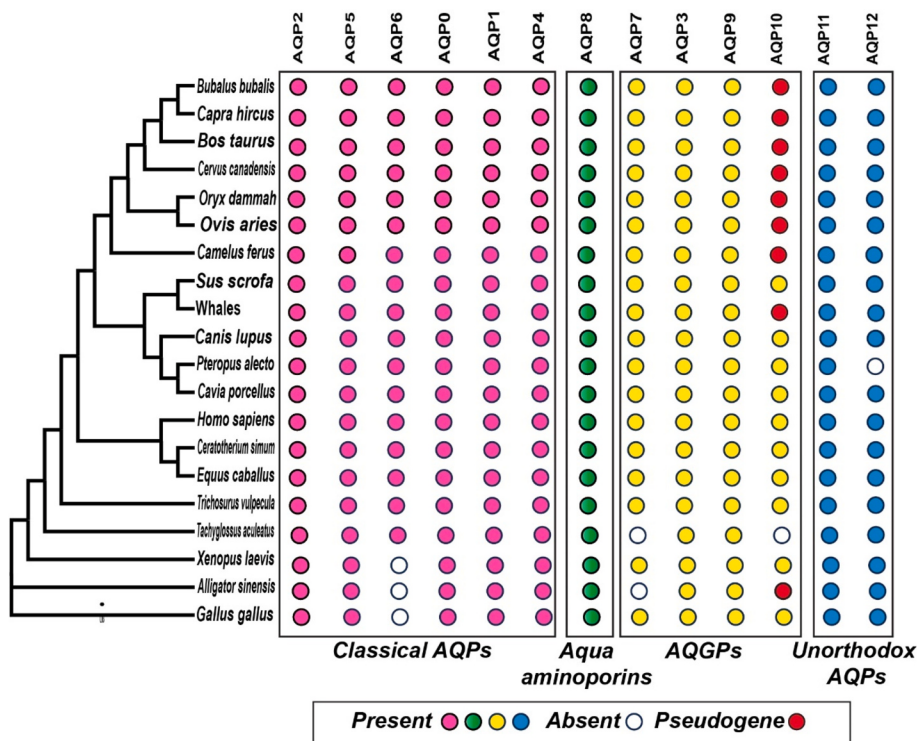


Fig. 2. Divergence of AQPs in 20 vertebrate species. AQP0, 1, 2, 3, 4, 8, 9, and 11 are present in all vertebrate species. Some species of artiodactyla (camel); crocodilia (alligator); anura (frogs), Galliformes (chickens), monotremes, and marsupials lack AQP5 (4.5 kb), AQP6 (2.5 kb), AQP7, AQP10, or AQP12 genes. Abbreviations: AQPs (Aquaporins); AQGPs (Aquaglyceroporins).

substituted three bases at 3 genomic stop codon of Exon8; *Alligator sinensis* (crocodile: XM_025212639.1: two bases inserted in one codon of Exon8).

The above-mentioned frameshift mutations due to insertions and deletions could be caused by sequencing errors. To confirm the indels of AQP10 in ruminants including buffalo, cattle, goat, and sheep, we obtained their sequence. The sequences confirmed the presence of indels due to which a premature termination occurred (Fig. 4). We found an insertion of GT residues in exon7 of buffalo AQP10, likewise a deletion of TCT and AG was observed in exon7 of buffalo and cattle (Fig. 4). We also found a deletion of TCT and C residues from exon6 and exon5 of goat and sheep respectively (Fig. 4). Thus, AQP10 gene of ruminants and other artiodactyla species except for *Sus scrofa*, is a pseudogene as it cannot produce a functional protein even if it is translated. The comparison of AQP10 between rodents and artiodactyls revealed that *Rattus norvegicus* and other rodents have maintained their coding frame. However, AQP10 has become a pseudogene in artiodactyls and certain rodent species like mice (Fig. S4).

3.6. Evolutionary analysis of AQPs

A total of 248 protein sequences of AQPs from 20 vertebrate species were used to build a rooted phylogenetic tree with *C. elegans* as an outgroup. This dataset was subjected to maximum likelihood analysis using RAxML, which recovered 13 AQP classes divided into four major clusters based on the variability of their amino acids, including AQP8 aqua-ammoniaporins, classical AQPs (AQP2, 5, 6, 0, 1, and 4), aquaglyceroporins (AQP3, 7, 9, and 10), and unorthodox AQPs (AQP11 and 12) (Figs. 5 and S5). The molecular phylogenetic analysis showed that the AQP genes of the same order tend to cluster together than to other orders, which was consistent with their traditional taxonomic groupings. In each cluster, AQP genes of ruminants (artiodactyla) were most closely related to whales (artiodactyla), rhinos and equines (perissodactyla). Phylogenetically, AQP genes of reptiles (crocodile) clustered

together with birds (chicken), which is closer to the amphibians; marsupials and monotremes formed independent clades; primates, rodents, and carnivores cluster in another clade (Figs. 5 and S5).

Gene duplication enables the divergent evolution of the resulting gene copies, enabling novel protein functions and patterns of gene expression. In our study, we found a total of 11 internal nodes in the AQP gene family where duplication occurred, which is presented as a closed blue diamond in the gene tree (Fig. S6). The gene tree shows that a significant duplication occurred between AQP8 and the rest of AQP types. Within Classical AQPs, AQGPs and Unorthodox type of AQPs, a total of 5, 3, and 1 internal node may have experienced the duplication events, which led to the expansion of AQP gene family (AQP0–12) in vertebrates. In classical aquaporins, an ancestral duplication of AQP0 gene led to the formation of three new classes including AQP2, 5, and 6, unique to vertebrates, whereas in AQGPs, duplication of AQP3 led to the emergence of other AQGPs.

3.7. Detection of positive selection at amino acids of AQPs

To determine the sites under positive selection in AQPs, each clade of artiodactyla, perissodactyla, primates, chiroptera, rodentia, carnivora, diprotodontia, monotremes, galliformes, anura, and crocodilia were selected as the foreground lineage in each case, to calculate the ω (dN/dS) values. The branch-site models using the BEB test with $PP > 0.95$ (LRT p-value < 0.05 and $\omega > 1$) identified a total of 6; 3; 16; 5; 32; 5, 2, and 54 positively selected sites in different lineages of AQP0, AQP2, AQP3, AQP6, AQP7, AQP8, AQP9, and AQP10 respectively. The LRT p-value (< 0.05) that are significant for the selected lineages remained significant after test correction (FDR-test) with Q-value < 0.05 . The detailed information is listed in Table 1.

To understand the impact of positively selected sites, the nature and location of substitutions among these sites were determined and subsequently mapped on the tertiary structure of AQPs. The results revealed that some sites were associated with non-synonymous substitutions,

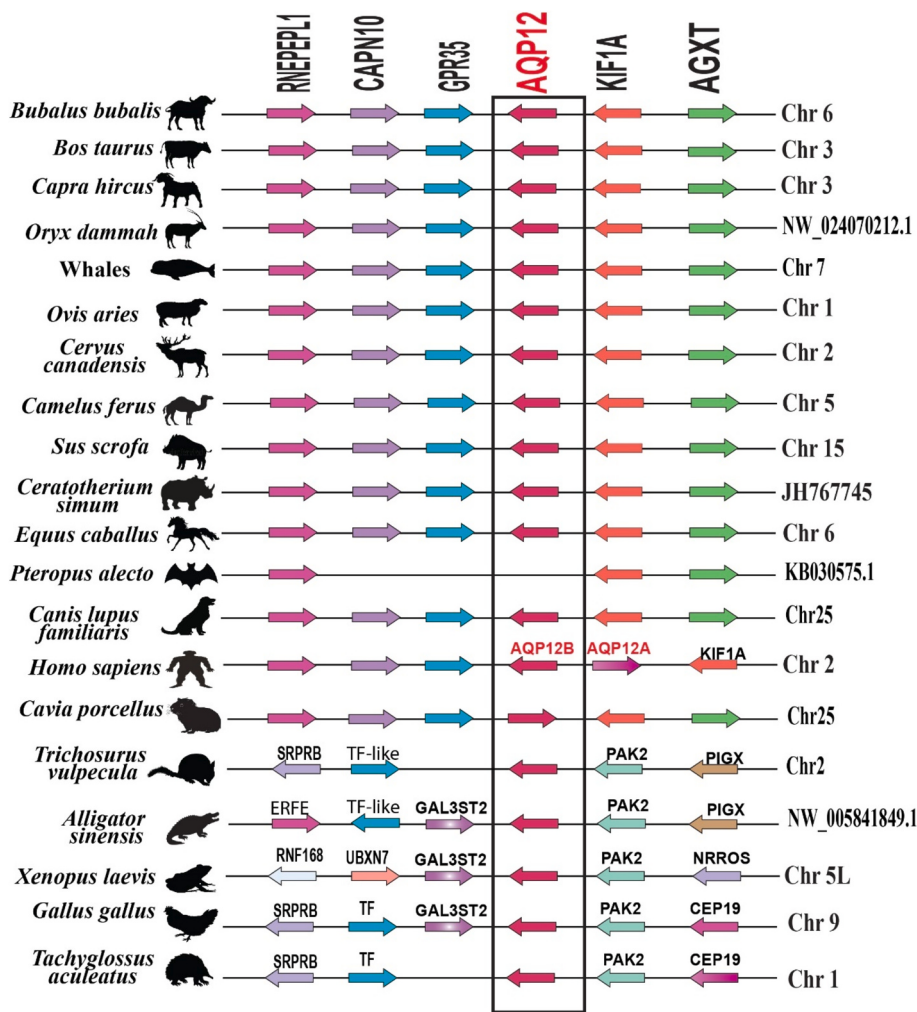


Fig. 3. Syntenic location of the AQP12 gene in artiodactyla and its related species. The AQP12 gene and the neighbouring genes are represented by different colour arrows. The orientation of arrowheads shows the direction of the gene structure. Genes are mapped based on their actual position in the genome (UCSC genome browser and NCBI Genome Viewer).

observed at the N-terminal end, inner membrane, and in proximity to critical residues such as the NPA motif and ar/R selectivity filter (Fig. 6). The detailed information is listed in Table S11.

3.8. Molecular docking analysis

The results of molecular docking indicated that certain amino acid residues in both AQP3 and AQP7 interact with glycerol. Specifically, Y150, G207 in AQP3; and H92, L97 and G187 in AQP7. Significant interactions were observed with urea at critical residues such as G145, A148 in AQP3, and Y223, R229 in AQP7. The ligand DFP00173 (inhibitor) exhibited a higher affinity of -7.3 and -6.2 (kcal/mol) at G79, A80; and G90 of AQP3 and 7 respectively. Meanwhile, the ligand Z433927330 (inhibitor) demonstrated stronger binding affinity of -9.5 and -8.6 (kcal/mol) at A80, N83 of AQP3; and A91, H92 of AQP7 (Figs. S7 and S8). The binding affinity and the common amino acid residues involved in hydrogen bond interactions are represented in Table S12.

3.9. Expression of AQP genes in buffalo and goat

AQPO, 1, 2, 4, 5, and 6 are classified as water-selective classical aquaporins. The tissue expression analysis indicated that AQP0 gene was strongly expressed in buffalo and goat eye lens with moderate expression observed in lymph node, testis, and rumen of buffalo (Figs. 7–8 and S9). The gene for AQP1 was widely distributed in different tissues and

cells of buffalo and goat, with majority being expressed in kidney, heart, spleen, and small intestine of buffalo; and rumen and liver tissues in goat. The AQP2 and AQP6 gene were predominantly expressed in buffalo and goat kidney. Our results also showed that AQP4 gene was highly expressed in buffalo brain and bone marrow tissue with moderate expression observed in heart, spleen, tongue, and macrophages; whereas goat AQP4 was strongly expressed in spleen and rumen tissues. AQP5 gene was abundant in rumen, and macrophage cells of buffalo and goat, whereas less expression was observed in eye lens, brain, bone marrow, heart, liver, lymph node, spleen, testis, tongue, and tonsils (Figs. 7–8 and S9).

AQGPs are another subtype of AQPs consisting of AQP3, 7, 9 and 10 genes. The present study revealed wide distribution of the AQP3 gene, majorly being expressed in the spleen, rumen, and neutrophils, with moderate expression observed in the brain, heart, kidney, liver, pancreas, lymph node, eye, small intestine, tongue, tonsils, and macrophages of buffalo and goat (Figs. 7–8 and S9). The AQP7 was highly expressed in buffalo and goat testis with moderate expression observed in heart. The AQP9 gene was predominantly expressed in buffalo monocyte cells, testis, and liver tissues, whereas it was highly expressed in goat liver. From our cloning and sequencing results, we found AQP10 as a pseudogene, hence we were unable to detect AQP10 gene expression (Figs. 7–8 and S9).

AQP8, AQP11 and AQP12 are classified as aqua-ammoniaporins and unorthodox AQPs respectively. Our results indicated the higher

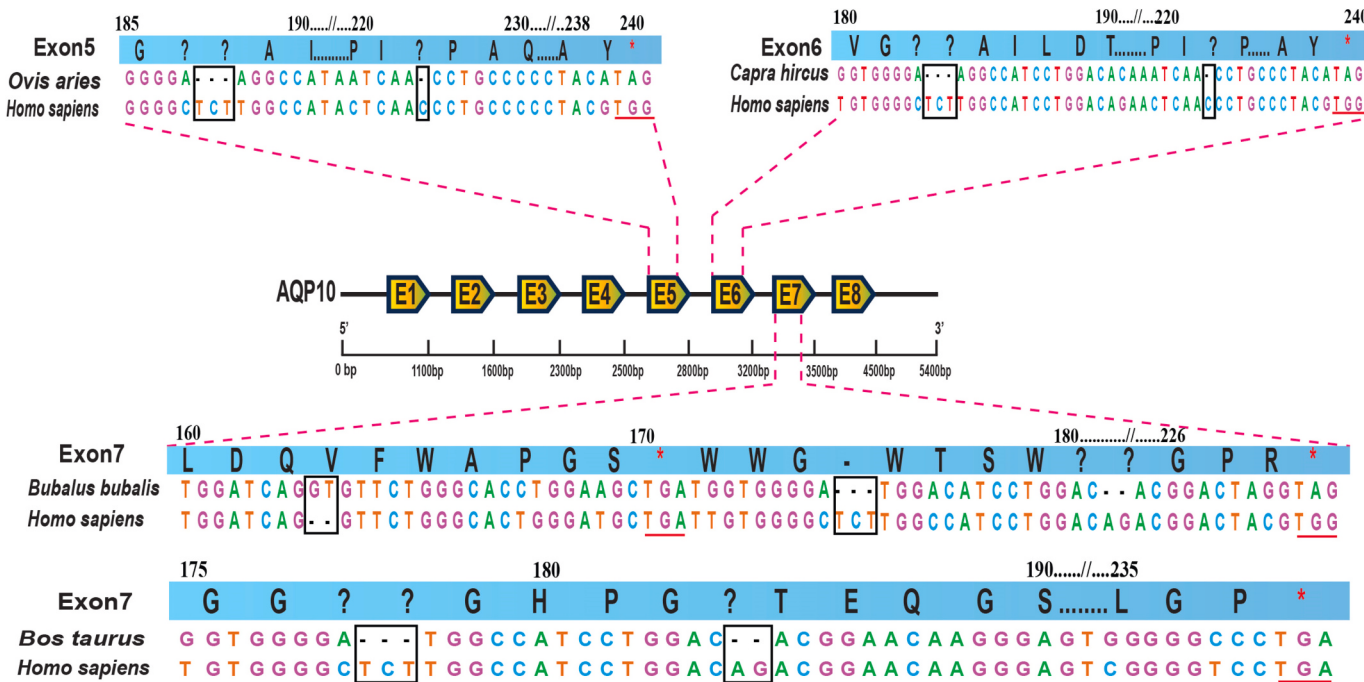


Fig. 4. Frame shift mutation in AQP10 of ruminants. (i) Deletion of TCT and C residues from Exon5 and Exon6 in sheep and goat; (ii) An insertion of GT and deletion of TCT and AG was observed in Exon7 of buffalo and cattle. Indels are shown in black boxes and stop codon are underlined.

expression of *AQP8* in buffalo and goat testis and liver tissues, on the other hand, *AQP11* was widely expressed in all tissues and cells of buffalo and goat, but highly expressed in buffalo whole blood cells (WBCs) and testis; and moderately expressed in other tissues. Similarly, *AQP11* was abundant in goat testis tissue (Figs. 7–8 and S9). We observed least expression of *AQP12* across different tissues in buffalo, whereas moderate expression was observed in eye lens, tongue and tonsils in goat (Figs. 7–8).

4. Discussion

The present investigation provides a comprehensive understanding of Aquaporins (AQPs) in buffalo and goat, encompassing their characterization, organization, transcript variants, pseudogenization, evolutionary analysis, and widespread distribution across tissues. This study presents the first evidence of the characterization, and expression analysis of the *AQP* gene family in buffalo and goat. A total of 13 full length *AQP* genes were successfully cloned and characterized in both species. Based on both the phylogenetic analysis and biological characteristics, AQPs paralogs were classified into four subfamilies: six classical AQPs, four aquaglyceroporins (AQGPs), two unorthodox AQPs, and one aqua-ammoniaporins (*AQP8*-type), which aligns with the previous studies [36,56–58]. The evolutionary analysis strongly supports the sister group relationship between *AQP0* and the *AQP2+AQP6+AQP5* clade of classical aquaporins; and a similar relationship was observed in previous studies on AQGs [59].

The meticulous analysis showed *AQP* gene losses in various vertebrates, indicating species specific losses. For instance, *AQP6* is absent in amphibians, alligator, and birds, indicating that other AQPs such as *AQP2* and *AQP5*, which are located on the same chromosome, might compensate for its function. Additionally, *AQP12* is absent in certain mammals such as *Pteropus alecto*. This suggests that evolutionary pressures like changes in habitat, diet, or physiological demands influence the gain or loss of AQPs. A notable example of gene loss is the *GULO* gene in humans, apes, bats, mice, rats, birds, and pigs due to the loss of function mutations in the L-gulonolactone oxidase enzyme, impacting the natural production of vitamin C in the body [60]. In contrast, all 13

AQP paralogs remained conserved in ruminants like buffalo, goat, cattle, and sheep. The conserved gene paralogs are required for the accomplishment of specialized physiological functions. For instance, the HSP and MHC gene paralogs encode numerous vital functions that play an imperative role in thermotolerance and controlling the vertebrate adaptive immunity, respectively [61,62]. In addition to different paralogs, the present study revealed the presence of transcript variants in buffalo and goat AQPs, that could be generated through alternative splicing mechanisms, altering protein function [63]. Previous studies have reported novel transcript variants for *AQP1*, *AQP3*, *AQP4*, and *AQP11* resulting from exon skipping in human, mouse, rat, chicken, and invertebrates [64,65]. The NPA motifs and ar/R residues represent highly conserved signature of AQPs, crucial for pore structure and function [66]. Our study revealed that some variants of goat *AQP5* and *AQP6* lacked important water transport NPA motifs, located at the C-terminal end. The absence of YRLL motif in rhesus monkey *AQP3* and human *AQP10* has been reported to impact the basolateral protein sorting in the epithelial cells [64,67]. We hypothesize that variants lacking NPA motifs and other important residues may impact the pore structure and water transport function. Genetic transcript variants of AQPs may result in the disturbance of the formation of tetramers, faulty sorting of AQPs, misfolding or other dysfunctions [25].

AQPs may lose function through gene duplications, as observed with *AQP7* in humans and *AQP10* in rodents, both identified as pseudogenes [31,32,68]. Pseudogenes usually arise from the decay of genes that have evolved through gene duplications. These tandemly duplicated genes turn to a pseudogene while one of them preserve its original function [69]. For instance, humans possess authentic *AQP7* gene alongside several pseudogenes like *AQP7L1*, located in the centromeric region of Chromosome 2, and *AQP7p1-7p5* [70,71]. However, the absence of functional *AQP10* gene in artiodactyla species suggests that the function of *AQP10* may not be crucial for their survival and its function may be compensated by other aquaglyceroporins. [32]. *AQP10* has been identified as a pseudogene in cattle, sheep, goat, and mice in previous studies [31,32]. Our study extends this finding by revealing that *AQP10* is a pseudogene across all artiodactyls including ruminants except swine and some rodents. The gene sequence analysis revealed numerous mutations

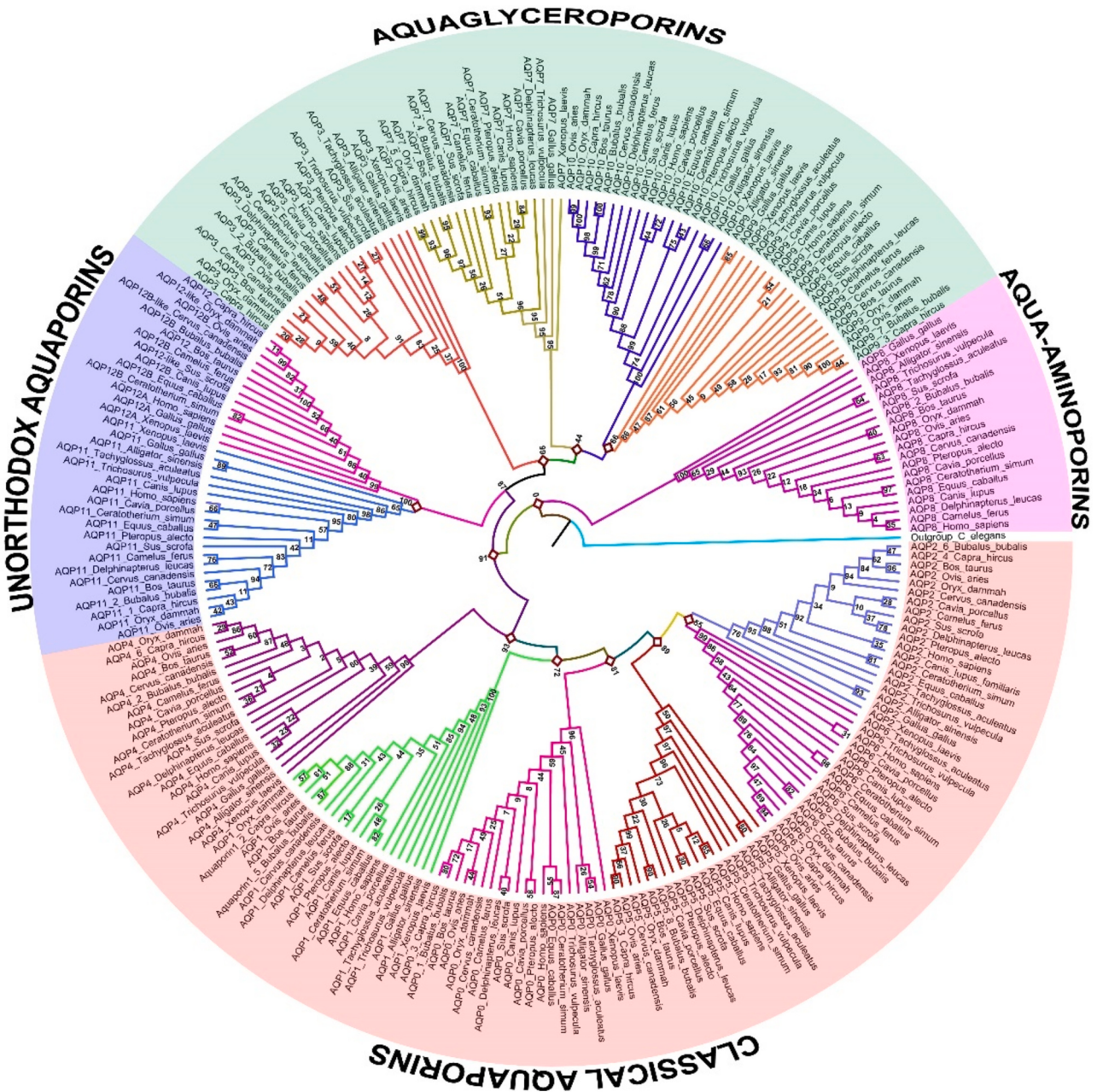


Fig. 5. Phylogenetic tree of the 20 vertebrate AQPs. The maximum likelihood tree of 248 protein sequences was constructed using RAxML software version 8.2.10 based on the best-fitted protein substitution GTR + GAMMA (general time reversible) model. Values at nodes represent boot-strap values. The Maximum Likelihood based phylogenetic tree forms four clusters, including Classical AQPs, Aquaglyceroporins, Unorthodox AQPs, and Aqua-ammoniaporins.

near the active sites in the *AQP10* gene, likely caused by insertions and deletions that result in the frame-shifts and splice junction mutations [31,32]. The degree of mutations in the bovine *AQP10* was found more compared to the murine *AQP10* gene, with both unrelated to each other. Since pseudogenes lack functional constraints, they generally accumulate more mutations than the functional genes [32]. It is possible that the *AQP10* gene may have turned into a pseudogene in ruminants that rechew and regurgitate their food, long before when bovines and their close relatives evolved from porcine ancestors [72]. In cetartiodactyla, the C-terminal fragment of the aquaporin gene contains a premature stop codon that results in truncated protein [57]. This highlights that the extent of aquaporin pseudogene is large and beyond ruminants.

The evidence of positive selection in the artiodactyla lineage of AQP2 coincided with previous findings, which suggested that these lineages

may have diverse osmoregulation abilities to adapt in distinct environments related to different feeding habitats [26,73,74]. Positive selection of AQP3 in the chiroptera and carnivora lineages at N-terminal positions 14, 31, and 34 may result in stronger binding of the N-terminal domain to the surfactant phospholipid layer and increased adsorption of the protein to the air-liquid interface [75]. This confers high water permeability to different layers of the epidermis, suggesting adaptations to cold stress and harsh environments [73,74,76]. A strong positive selection in the artiodactyla lineage of AQP7 gene at sites 222, 226, 227, and 232, located at or near NPA motifs and ar/R selectivity filter, consequently affects the solute selectivity, pore formation and protein function, suggesting adaptation [56,74]. Ghoreishifar and co-workers found strong evidence of positive selection in the AQP3 and AQP7 gene in swedish cattle, suggesting important role in cold acclimation

Table 1Results of branch-site models that are significant (Q Value < 0.05 and $\omega > 1$) in the foreground branches.

S.No.	Aquaporins	Foreground branch	Model compared	Estimates of parameters	LRT-p value	Q value	Positively selected sites
1.	AQPO	Alligator	Model A (np = 40)	P0 = 0.85788 P1 = 0.07437 Model A null (np = 39) (P2a + P2b = 0.06774) $\omega_0 = 0.06014$ $\omega_1 = 1.00000$ $\omega_2 = 35.02694$	0.000004214	6.55511E-06	104 L 0.997**, 105 Y 0.996**, 108 T 0.998**, 111 A 0.998**, 112 N 0.998**, 113 T 0.997**
			Vs				
			Model A null (np = 39)				
		Chicken	Model A (np = 40)	P0 = 0.85788 P1 = 0.07437 Model A null (np = 39) (P2a + P2b = 0.06774) $\omega_0 = 0.06014$ $\omega_1 = 1.00000$ $\omega_2 = 35.02658$	0.000004214	5.8996E-06	(P > 95 %)
			Vs				
			Model A null (np = 39)				
	AQP2	<i>Cervus clade</i>	Model A (np = 42)	P0 = 0.82788 P1 = 0.12919 Model A null (np = 41) (P2a + P2b = 0.04292) $\omega_0 = 0.04611$ $\omega_1 = 1.00000$ $\omega_2 = 264.42516$	0.000000000	0	213 Q 1.000**, 216 E 1.000**, 224 P 0.998** (P > 95 %)
			Vs				
			Model A null (np = 41)				
		<i>Delphinapterus leucas</i>	Model A (np = 42)	P0 = 0.82788 P1 = 0.12919 Model A null (np = 41) (P2a + P2b = 0.04292) $\omega_0 = 0.04611$ $\omega_1 = 1.00000$ $\omega_2 = 264.42396$	0.000000011	4.76667E-08	
			Vs				
			Model A null (np = 41)				
3.	AQP3	<i>Pteropus alecto</i>	Model A (np = 42)	P0 = 0.86161 P1 = 0.03189 Model A null (np = 41) (P2a + P2b = 0.1065) $\omega_0 = 0.03809$ $\omega_1 = 1.00000$ $\omega_2 = 809.54261$	0.000000000	0	2 G 1.000**, 3 R 0.999**, 4 Q 0.999**, 5 Q 1.000**, 14 M 0.996**, 15 L 0.999**, (P > 95 %)
			Vs				
			Model A null (np = 41)				
		<i>Canis lupus</i>	Model A (np = 42)	P0 = 0.86161 P1 = 0.03189 Model A null (np = 41) (P2a + P2b = 0.1065) $\omega_0 = 0.03809$ $\omega_1 = 1.00000$ $\omega_2 = 679.12810$	0.000000000	0	19 Y 1.000**, 20 R 0.996**, 22 L 0.983*, 28 E 0.998**, 30 L 0.999**, 31 G 0.999**, 33 L 0.998**, 34 I 1.000**, 35 L 0.988*, 36 V 0.999** (P > 95 %)
			Vs				
			Model A null (np = 41)				
4.	AQP6	<i>Canis lupus</i>	Model A (np = 34)	P0 = 0.70182 P1 = 0.20209 Model A null (np = 33) (P2a + P2b = 0.09608) $\omega_0 = 0.05264$ $\omega_1 = 1.00000$ $\omega_2 = 207.41674$	0.000000107	1.52857E-07	202 V 0.958*, 231 Q 0.989*, 235 I 0.997**, 238 G 0.999**, 239 S 0.997** (P > 95 %)
			Vs				
			Model A null (np = 33)				
		<i>Cavia porcellus</i>	Model A (np = 34)	P0 = 0.45397 P1 = 0.53377 Model A null (np = 33) (P2a + P2b = 0.09608) $\omega_0 = 0.05264$ $\omega_1 = 1.00000$ $\omega_2 = 207.41644$	0.000000107	1.3375E-07	
			Vs				
			Model A null (np = 33)				
4.	AQP7	<i>Bos clade</i>	Model A (np = 38)	P0 = 0.45834 P1 = 0.18341 Model A null (np = 37) (P2a + P2b = 0.35825) $\omega_0 = 0.08716$ $\omega_1 = 1.00000$ $\omega_2 = 685.20124$	0.000000000	0	178 V 0.993**, 179 T 0.988*, 192 K 0.993**, 194 N 1.000**, 195 N 1.000**, 199 L 0.988*, 200 G 1.000**, 201 T 0.989*, 202 Q 0.981*, 203 A 1.000**, 205 M 1.000**, 220 N 1.000**, 222 G 0.988*, 223 Y 1.000**, 224 A 0.972*, 225 I 0.991**, 226 N 1.000**, 227 P 0.987*, 228 S 0.984*, 229 R 0.641, (continued on next page)
			Vs				
			Model A null (np = 37)				
		<i>Oryx Clade</i>	Model A (np = 38)	P0 = 0.45834 P1 = 0.18341 Model A null (np = 37) (P2a + P2b = 0.01668) $\omega_0 = 0.00500$ $\omega_1 = 1.00000$ $\omega_2 = 687.13177$	0.000000000	0	200 G 1.000**, 201 T 0.989*, 202 Q 0.981*, 203 A 1.000**, 205 M 1.000**, 220 N 1.000**, 222 G 0.988*, 223 Y 1.000**, 224 A 0.972*, 225 I 0.991**, 226 N 1.000**, 227 P 0.987*, 228 S 0.984*, 229 R 0.641,
			Vs				
			Model A null (np = 37)				

Table 1 (continued)

S.No.	Aquaporins	Foreground branch	Model compared	Estimates of parameters	LRT-p value	Q value	Positively selected sites
5.	AQP8	<i>Delphinapterus leucas</i>	Model A (np = 42)	P0 = 0.80731 Vs Model A null (np = 41)	0.000000000	0	230 D 1.000**, 232 P 0.993**, 233 P 1.000**, 234 R 1.000**, 235 F 0.987*, 236 F 1.000*, 237 T 0.986*, 237 F 0.954*, 240 A 1.000**, 241 R 0.968*, 243 G 0.987*, 246 V 0.973* (P > 95 %)
			Model A (np = 42)	P0 = 0.80731 Vs Model A null (np = 41)	0.000000000	0	273 D 0.992**, 275 K 0.996**, 276 I 0.994**, 277 R 0.992**, 278 K 0.998** (P > 95 %)
			Equus clade	P0 = 0.80731 Vs Model A null (np = 41)	0.000000000	0	273 D 0.992**, 275 K 0.996**, 276 I 0.994**, 277 R 0.992**, 278 K 0.998** (P > 95 %)
			Model A (np = 42)	P0 = 0.80731 Vs Model A null (np = 41)	0.000000000	0	273 D 0.992**, 275 K 0.996**, 276 I 0.994**, 277 R 0.992**, 278 K 0.998** (P > 95 %)
			Model A (np = 42)	P0 = 0.80731 Vs Model A null (np = 41)	0.000000000	0	273 D 0.992**, 275 K 0.996**, 276 I 0.994**, 277 R 0.992**, 278 K 0.998** (P > 95 %)
		<i>Trichosurus vulpecula</i>	Model A (np = 42)	P0 = 0.71668 Vs Model A null (np = 41)	0.001577852	0.001699225	129 M 0.962*, 211 S 0.974* (P > 95 %)
			Model A (np = 42)	P0 = 0.71668 Vs Model A null (np = 41)	0.001577852	0.001577852	129 M 0.962*, 211 S 0.974* (P > 95 %)
			Model A (np = 42)	P0 = 0.71668 Vs Model A null (np = 41)	0.001577852	0.001577852	129 M 0.962*, 211 S 0.974* (P > 95 %)
			Model A (np = 42)	P0 = 0.71668 Vs Model A null (np = 41)	0.001577852	0.001577852	129 M 0.962*, 211 S 0.974* (P > 95 %)
			Model A (np = 42)	P0 = 0.71668 Vs Model A null (np = 41)	0.001577852	0.001577852	129 M 0.962*, 211 S 0.974* (P > 95 %)
6.	AQP9	<i>Homo sapiens</i>	Model A (np = 42)	P0 = 0.50499 Vs Model A null (np = 41)	0.027603693	0.035884801	Not allowed (P > 95 %)
			Model A (np = 42)	P0 = 0.50499 Vs Model A null (np = 41)	0.027603693	0.029904001	Not allowed (P > 95 %)
			Model A (np = 42)	P0 = 0.50499 Vs Model A null (np = 41)	0.027603693	0.029904001	Not allowed (P > 95 %)
			Model A (np = 42)	P0 = 0.50499 Vs Model A null (np = 41)	0.027603693	0.029904001	Not allowed (P > 95 %)
			Model A (np = 42)	P0 = 0.50499 Vs Model A null (np = 41)	0.027603693	0.029904001	Not allowed (P > 95 %)
		<i>Bubalus</i> clade	Model A (np = 28)	P0 = 0.83021 Vs Model A null (np = 27)	0.008254572	0.04127286	51 G 0.978* (P > 95 %)
			Model A (np = 28)	P0 = 0.83021 Vs Model A null (np = 27)	0.008254572	0.016509144	51 G 0.978* (P > 95 %)
			Model A (np = 28)	P0 = 0.83021 Vs Model A null (np = 27)	0.008254572	0.016509144	51 G 0.978* (P > 95 %)
			Model A (np = 28)	P0 = 0.83021 Vs Model A null (np = 27)	0.008254572	0.016509144	51 G 0.978* (P > 95 %)
			Model A (np = 28)	P0 = 0.83021 Vs Model A null (np = 27)	0.008254572	0.016509144	51 G 0.978* (P > 95 %)
8.	AQP12	<i>Ovis</i> clade	Model A (np = 28)	P0 = 0.83021 Vs Model A null (np = 27)	0.008254572	0.04127286	51 G 0.978* (P > 95 %)
			Model A (np = 28)	P0 = 0.83021 Vs Model A null (np = 27)	0.008254572	0.016509144	51 G 0.978* (P > 95 %)
			Model A (np = 28)	P0 = 0.83021 Vs Model A null (np = 27)	0.008254572	0.016509144	51 G 0.978* (P > 95 %)
			Model A (np = 28)	P0 = 0.83021 Vs Model A null (np = 27)	0.008254572	0.016509144	51 G 0.978* (P > 95 %)
			Model A (np = 28)	P0 = 0.83021 Vs Model A null (np = 27)	0.008254572	0.016509144	51 G 0.978* (P > 95 %)
		<i>Camelus ferus</i>	Model A (np = 28)	P0 = 0.82960 Vs Model A null (np = 27)	0.029622107	0.042317296	Not allowed (P > 95 %)
			Model A (np = 28)	P0 = 0.82960 Vs Model A null (np = 27)	0.029622107	0.042317296	Not allowed (P > 95 %)
			Model A (np = 28)	P0 = 0.82960 Vs Model A null (np = 27)	0.029622107	0.042317296	Not allowed (P > 95 %)
			Model A (np = 28)	P0 = 0.82960 Vs Model A null (np = 27)	0.029622107	0.042317296	Not allowed (P > 95 %)
			Model A (np = 28)	P0 = 0.82960 Vs Model A null (np = 27)	0.029622107	0.042317296	Not allowed (P > 95 %)
9.	AQP13	<i>Gallus gallus</i>	Model A (np = 28)	P0 = 0.82960 Vs Model A null (np = 27)	0.007046938	0.008808673	
			Model A (np = 28)	P0 = 0.82960 Vs Model A null (np = 27)	0.007046938	0.008808673	
			Model A (np = 28)	P0 = 0.82960 Vs Model A null (np = 27)	0.007046938	0.008808673	
			Model A (np = 28)	P0 = 0.82960 Vs Model A null (np = 27)	0.007046938	0.008808673	
			Model A (np = 28)	P0 = 0.82960 Vs Model A null (np = 27)	0.007046938	0.008808673	
10.	AQP14	<i>Homo sapiens</i>	Model A (np = 28)	P0 = 0.82960 Vs Model A null (np = 27)	0.029622142	0.032913491	
			Model A (np = 28)	P0 = 0.82960 Vs Model A null (np = 27)	0.029622142	0.032913491	
			Model A (np = 28)	P0 = 0.82960 Vs Model A null (np = 27)	0.029622142	0.032913491	
			Model A (np = 28)	P0 = 0.82960 Vs Model A null (np = 27)	0.029622142	0.032913491	
			Model A (np = 28)	P0 = 0.82960 Vs Model A null (np = 27)	0.029622142	0.032913491	

(continued on next page)

Table 1 (continued)

S.No.	Aquaporins	Foreground branch	Model compared	Estimates of parameters	LRT-p value	Q value	Positively selected sites
		<i>Xenopus laevis</i>	Model A (np = 28) Vs Model A null (np = 27)	P0 = 0.73953 P1 = 0.14340 (P2a + P2b = 0.11707) ω_0 = 0.14340 ω_1 = 1.00000 ω_2 = 201.48400	0.007046938	0.007046938	
9.	AQP10	<i>Bos taurus</i>	Model A (np = 18) Vs Model A null (np = 17)	P0 = 0.53063 P1 = 0.18502 (P2a + P2b = 0.28435) ω_0 = 0.27691 ω_1 = 1.00000 ω_2 = 999.00000	0.000000000	0	11 K 0.992** 15 G 0.995** 19 R 0.994** 21 T 0.996** 22 S 0.989* 24 G 0.973* 129 Q 0.999** 130 Q 0.992** 142 P 0.959* 194 E 0.998** 195 Q 0.963* 197 S 0.998** 198 A 0.959* 199 C 0.999** 200 R 0.993** 201 S 0.997** 202 G 0.954* 204 C 1.000** 205 G 0.970* 206 S 1.000** 208 V 0.989* 209 T 0.999** 210 D 0.998** 211 P 0.954* 213 R 0.997** 214 H 0.999** 215 A 0.998** 216 I 0.998** 217 H 1.000** 219 C 0.994** 220 Q 0.998** 221 L 0.999** 228 C 0.998** 230 G 0.993** 234 T 0.996** 235 A 0.996** 237 H 0.996** 238 L 0.998** 239 R 0.995** 240 S 0.993** 241 W 0.973* 242 L 0.972* 246 S 0.976* 34 R 0.986* 35 Q 0.978* 37 L 0.999** 38 A 0.999** 84 V 0.958* 85 S 0.995** 87 N 0.997** 89 S 0.991** 238 L 0.997** 240 S 0.997** 246 S 0.993** (P > 95 %)
		<i>Mus musculus</i>	Model A (np = 18) Vs Model A null (np = 17)	P0 = 0.7023 P1 = 0.34186 (P2a + P2b = 0.08) ω_0 = 0.27691 ω_1 = 1.00000 ω_2 = 999.00000	0.000000000	0	129 Q 0.999** 130 Q 0.992** 142 P 0.959* 194 E 0.998** 195 Q 0.963* 197 S 0.998** 198 A 0.959* 199 C 0.999** 200 R 0.993** 201 S 0.997** 202 G 0.954* 204 C 1.000** 205 G 0.970* 206 S 1.000** 208 V 0.989* 209 T 0.999** 210 D 0.998** 211 P 0.954* 213 R 0.997** 214 H 0.999** 215 A 0.998** 216 I 0.998** 217 H 1.000** 219 C 0.994** 220 Q 0.998** 221 L 0.999** 228 C 0.998** 230 G 0.993** 234 T 0.996** 235 A 0.996** 237 H 0.996** 238 L 0.998** 239 R 0.995** 240 S 0.993** 241 W 0.973* 242 L 0.972* 246 S 0.976* 34 R 0.986* 35 Q 0.978* 37 L 0.999** 38 A 0.999** 84 V 0.958* 85 S 0.995** 87 N 0.997** 89 S 0.991** 238 L 0.997** 240 S 0.997** 246 S 0.993** (P > 95 %)

[77]. AQP3 and AQP7 genes facilitates glycerol, urea, and water transport, and are known to be associated with thermoregulation and altitude adaptations [78]. The hydrophobic to polar charged substitutions may significantly alter the substrate binding, consequently increasing the water permeability [73]. Liu and coworkers speculated that a single mutation of N60G in rat AQP6 can convert an anion-specific channel to a water selective channel [79,80]. The molecular docking studies identified that DFP00173 and Z433927330 binds at the critical amino acid residues of AQP3 and 7 with higher affinity which suggests that these could serve as therapeutic targets for various physiological conditions and diseases [81], however more experimental studies are required for

better understanding.

The gene expression of *AQP* gene family revealed that some *AQPs* were diversely present in various tissues and cells. *AQP0* was predominantly expressed in the eye lens of buffalo and goat, that emphasize the importance of this protein in maintaining lens integrity under various physiological conditions in bovines. Previous reports show that under thermal stress conditions, *AQP0* protein undergoes aggregation, thereby effecting the integrity of lens membrane in bovines [82,83]. The ubiquitous expression of *AQP1* and 3 in buffalo and goat, coincided with the previous findings in birds [26], mammals [25], and other vertebrates [84]. It has been reported that the ubiquitously expressed genes are

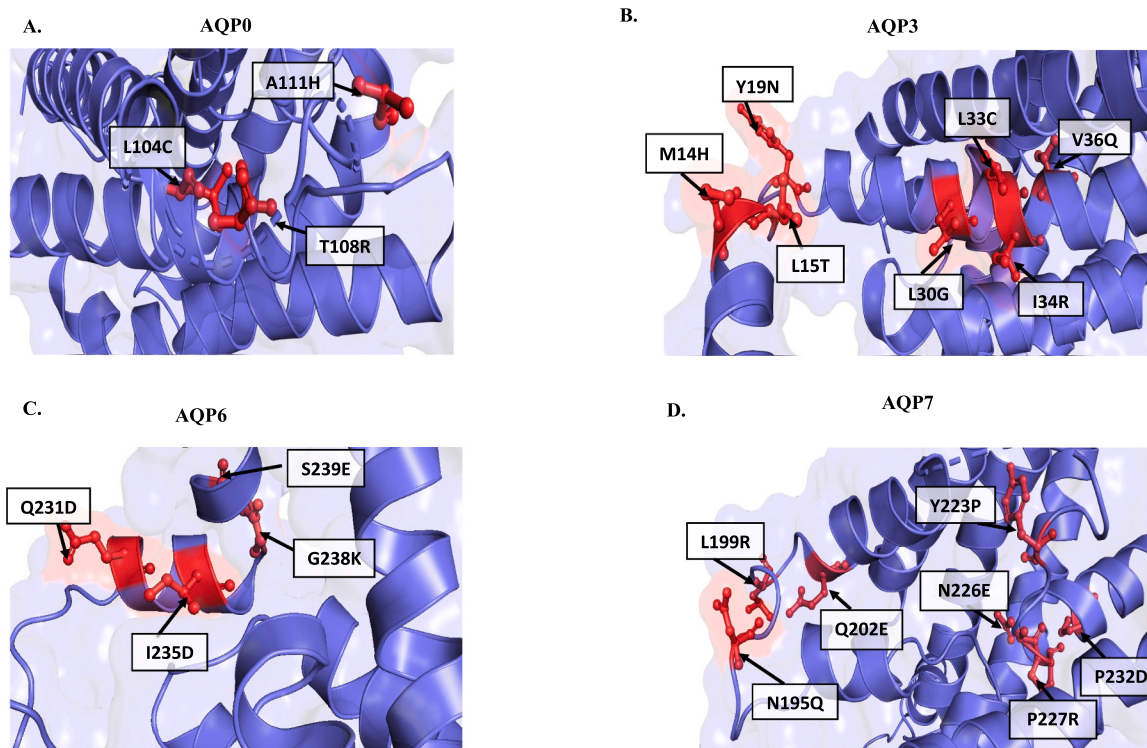


Fig. 6. Selection pressure analysis of AQPs using Branch-site models. A–D: The Monomeric protein structure of AQP0, 3, 6, and 7 with positively selected sites undergoing non-synonymous substitutions at active residues are depicted. The sites present near active residues are highlighted (red sticks) in tertiary protein structures.

more likely to have intracellular location and might be involved in macromolecule synthesis, transcription, and vesicles in human [26,85]. The tissue-specific expression of *AQP2* and *6* in the collecting duct of buffalo and goat kidney suggests possible involvement in tubular reabsorption function, thus preventing conditions like polyuria in animals [86,87]. The higher expression of *AQP3* in the buffalo and goat rumen epithelia, facilitates the export of urea down the concentration gradient, thus maintaining ruminant nitrogen balance [88]. Higher expression of *AQP3* in immune cells and tissues reveals an essential role for T-cell activation and regulates neutrophil and macrophage migration during sepsis [89]. *AQP4* expression in buffalo brain cells suggests the potential role of *AQP4* in maintaining brain homeostasis [66]. Costa and co-workers showed that overexpression of the *AQP4* gene in glial cells could cause an imbalance in water and ion homeostasis, thereby contributing to the usual histological abnormalities associated with bovine spongiform encephalopathies (BSE) [90]. Higher expression of *AQP5* gene in buffalo and goat macrophages suggests that *AQP5* is strongly associated with the activation of markers of B-cells, Th1 cells, and neutrophils, indicating its involvement in inflammation and innate immune response [91].

Expression of *AQP7*, *8*, and *9* gene in the buffalo and goat testis indicate its critical role in glycerol utilization that may act as an energy source for sperm motility and metabolism. Yeste and coworkers reported that sperm cells with high *AQP7* transcript levels in frozen thawed semen of bulls were positively correlated with sire conception rates, implying that these could withstand freezing and thawing better [92]. Higher expression of *AQP9* in testis suggests that it plays an important role in transepithelial water flow, which is necessary for maintaining

semen quality and reproductive fertility [93]. In the current study, *AQP11*, one of the unorthodox AQPs, was strongly expressed in testis and WBCs. Morato and coworkers revealed that the relative expression of *AQP11* in testis and both fresh and frozen spermatozoa is associated with the ability to survive osmotic stress and cryopreservation [94]. It is worthy of note that some AQPs such as *AQP0*, *2*, *4*, *5*, *7*, *8*, *9*, and *12* shows tissue restricted expression in buffalo and goat. On the other hand, some AQPs such as *AQP1*, *3*, and *11* are ubiquitously expressed.

5. Conclusion

In summary, we successfully sequenced *AQP* genes (*AQP0–11*) with coding regions spanning 729–990 bp in buffalo and goats. Comparative analysis revealed that ruminants maintain consistent number of aquaporin paralogs (13), while other vertebrates such as monotremes, marsupials, reptiles, and carnivores have a variable number of genes. Notably, *AQP3*, *5*, *6*, and *8* exhibited varying number of transcript variants, likely attributed to alternative splicing during transcription. The goat *AQP5* and *AQP6* transcript variants that lack NPA motifs and other critical regions may influence the aquaporin pore's structure and solute transport capabilities. *AQP10* of ruminants is a pseudogene within the artiodactyla lineage, but their function may be compensated by other AQPs. Positive selection at critical residues of *AQP0*, *3*, and *7* in artiodactyla, crocodilian, galliformes, chiroptera, carnivora, and rodentia lineages is accompanied by non-synonymous substitutions that could modify AQP structure and function, suggesting adaption to diverse environmental conditions. Tissue wide gene expression patterns of AQPs showed both ubiquitous and tissue-restricted expressions, thus

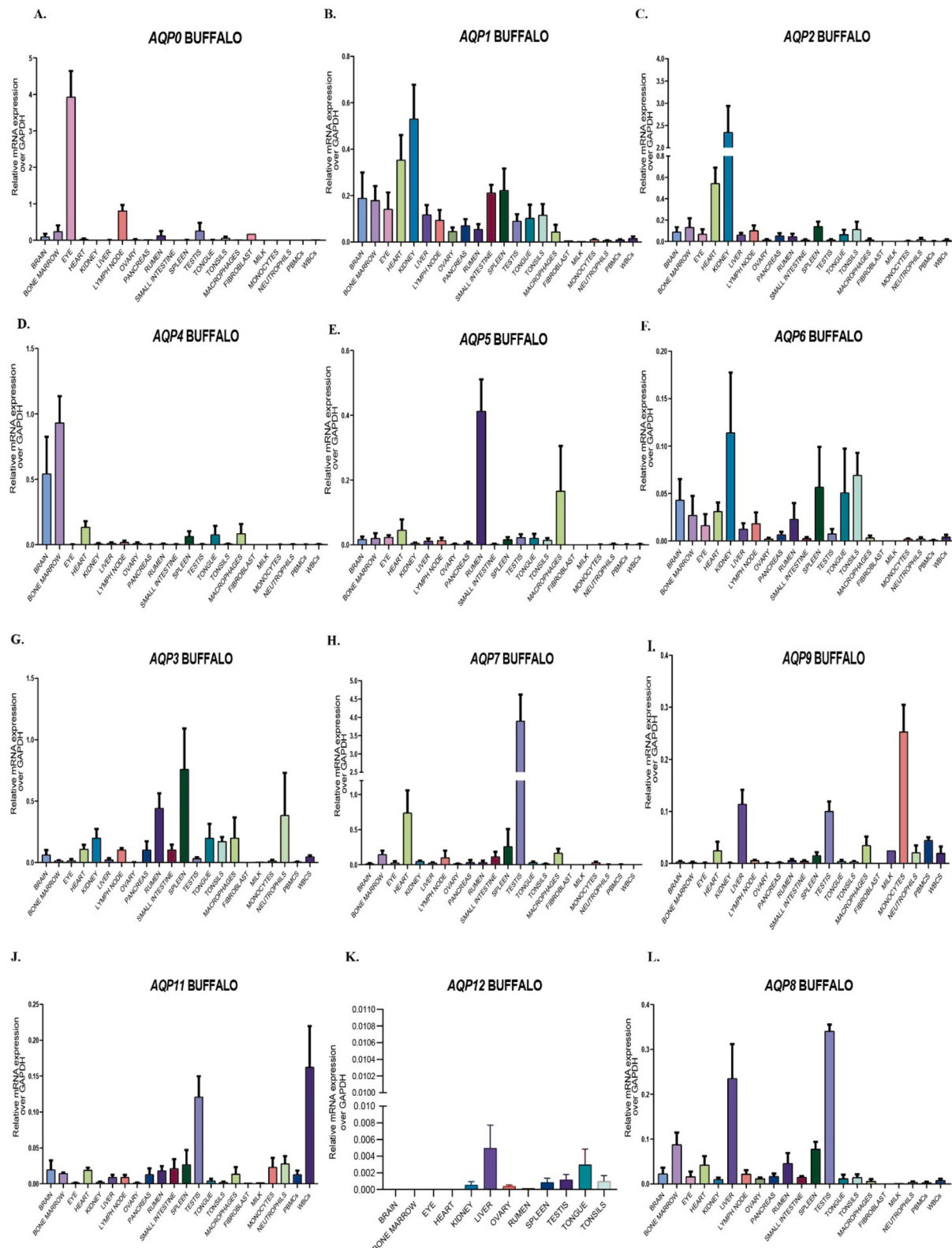


Fig. 7. Expression levels of AQPs in various tissues and cells of Buffalo (*Bubalus bubalis*). A–K: Expression of buffalo wAQPs (AQP0, 1, 2, 4, 5, and 6); AQGPs (AQP3, 7, 9), Unorthodox and Aqua-ammoniaporins (AQP11 and 8) were relative to GAPDH as a control. Each column represents the mean values \pm standard deviation from six biological replicates.

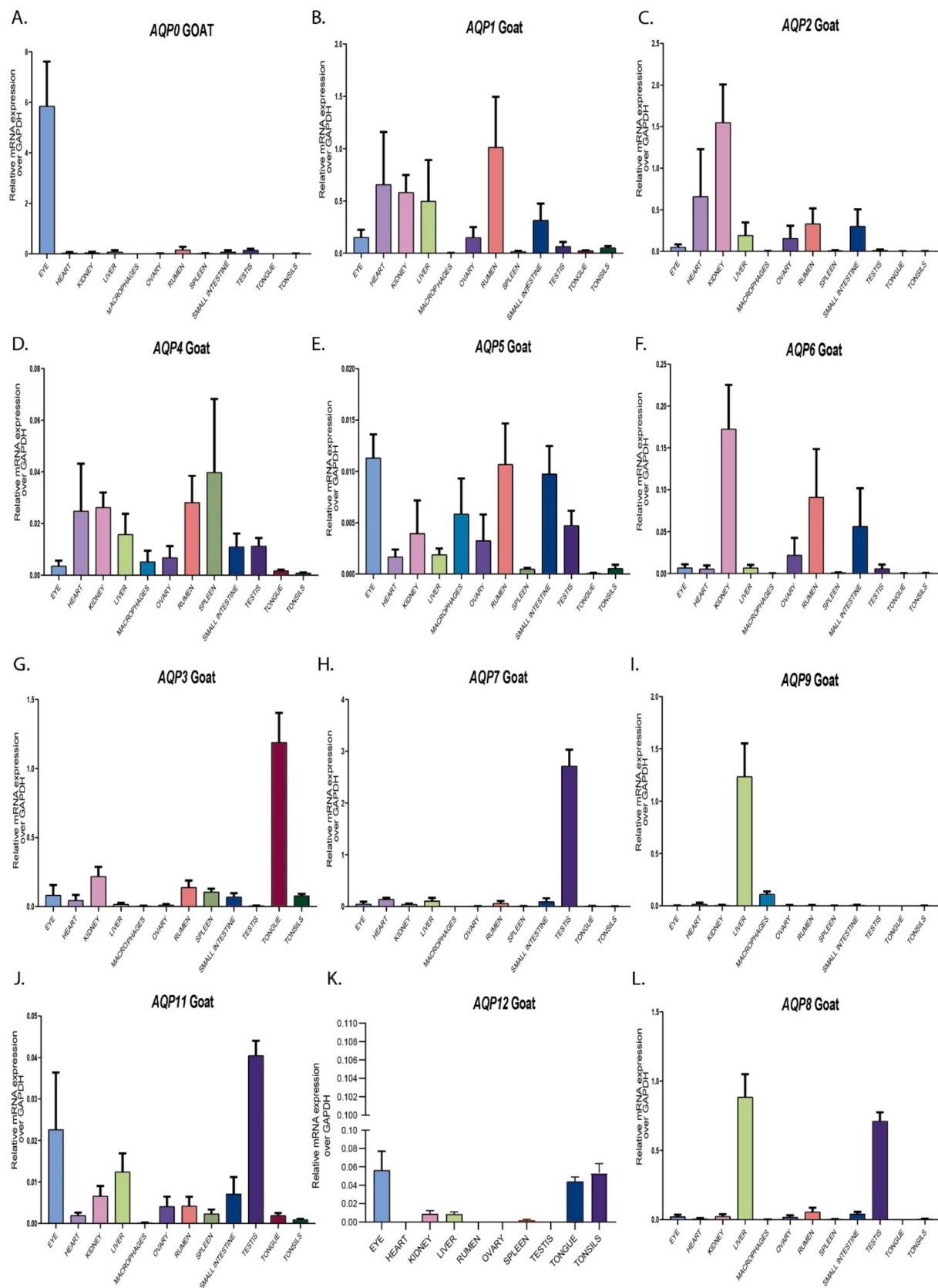


Fig. 8. Expression levels of AQPs in various tissues of Goat (*Capra hircus*). A–K: Expression of goat wAQPs (AQP0, 1, 2, 4, 5, and 6); AQGPs (AQP3, 7, 9), Unorthodox and aqua-ammoniaporins (AQP11 and 8) were relative to GAPDH as a control. Each column represents the mean values \pm standard deviation from six biological replicates.

indicating that AQP s may be implicated in distinct physiologies and pathophysiologies. This study not only contributes to a deeper understanding of AQP genes in ruminants, but also provides valuable foundation for future investigations aiming at molecular mechanism of AQP genes in response to various physiological conditions. More future studies are needed to confirm the impact of transcript variants and non-synonymous substitution on the AQP function.

Funding information

This work was supported by the ICAR - National Innovations in Climate Resilient Agriculture (NICRA) project.

CRediT authorship contribution statement

Shiveeli Rajput: Writing – review & editing, Writing – original draft, Visualization, Validation, Methodology, Investigation, Formal analysis, Data curation, Conceptualization. **Devika Gautam:** Writing – review & editing, Validation, Resources, Methodology, Investigation, Formal analysis, Conceptualization. **Ashutosh Vats:** Writing – review & editing, Validation, Resources, Methodology, Investigation, Formal analysis, Conceptualization. **Mayank Roshan:** Methodology, Resources. **Priyanka Goyal:** Resources. **Chanchal Rana:** Resources. **Payal S.M.:** Resources. **Ashutosh Ludri:** Supervision, Funding acquisition. **Sachinandan De:** Supervision, Funding acquisition, Conceptualization, Resources, Writing – review & editing.

Declaration of competing interest

The authors declare that they have read and approve the present manuscript and there is no known competing financial interests or personal relationships that could have appeared to influence the work reported in this paper.

Data availability

All the data analysed and generated in this study are included in this paper and its supplementary files.

Appendix A. Supplementary data

Supplementary data to this article can be found online at <https://doi.org/10.1016/j.ijbiomac.2024.136145>.

References

- [1] A. Markou, L. Unger, M. Abir-Awan, A. Saadallah, A. Halsey, Z. Baklava, M. Conner, S. Törnroth-Horsefield, S.D. Greenhill, A. Conner, R.M. Bill, M. M. Salman, P. Kitchen, Molecular mechanisms governing aquaporin relocation, *Biochim. Biophys. Acta - Biomembr.* 1864 (2022), <https://doi.org/10.1016/j.bbamem.2021.183853>.
- [2] Z. Wang, Y. Chen, C. Wang, N. Zhao, Z. Zhang, Z. Deng, Y. Cui, R. Wang, Y. Li, Aquaporins in Pacific white shrimp (*Litopenaeus vannamei*): molecular characterization, expression patterns, and transcriptome analysis in response to salinity stress, *Front. Mar. Sci.* 9 (2022) 119, <https://doi.org/10.3389/FMARS.2022.817868/BIBTEX>.
- [3] A.S. Verkman, M.O. Anderson, M.C. Papadopoulos, Aquaporins: important but elusive drug targets, *Nat. Rev. Drug Discov.* 13 (2014) 259–277, <https://doi.org/10.1038/nrd4226>.
- [4] P. Agre, Aquaporin water channels (nobel lecture), *Angew. Chemie - Int. Ed.* 43 (2004) 4278–4290, <https://doi.org/10.1002/anie.200460804>.
- [5] G. Calamita, J. Perret, C. Delporte, Aquaglyceroporins: drug targets for metabolic diseases? *Front. Physiol.* 9 (2018) <https://doi.org/10.3389/fphys.2018.00851>.
- [6] K. Ishibashi, Y. Tanaka, Y. Morishita, Perspectives on the Evolution of Aquaporin Superfamily, 1st ed., Elsevier Inc., 2020 <https://doi.org/10.1016/bv.vh.2019.08.001>.
- [7] A.K. Azad, T. Raihan, J. Ahmed, A. Hakim, T.H. Emon, P.A. Chowdhury, Human aquaporins: functional diversity and potential roles in infectious and non-infectious diseases, *Front. Genet.* 12 (2021), <https://doi.org/10.3389/fgene.2021.654865>.
- [8] R.N. Finn, J. Cerdá, Evolution and functional diversity of aquaporins, *Biol. Bull.* 229 (2015) 6–23, <https://doi.org/10.1086/BBLv229n1p6>.
- [9] R. Zardoya, Phylogeny and evolution of the major intrinsic protein family, *Biol. Cell* 97 (2005) 397–414, <https://doi.org/10.1042/bc20040134>.
- [10] F. Abascal, I. Irisarri, R. Zardoya, Diversity and evolution of membrane intrinsic proteins, *Biochim. Biophys. Acta - Gen. Subj.* 2014 (1840) 1468–1481, <https://doi.org/10.1016/j.bbagen.2013.12.001>.
- [11] M. Yeste, R. Morató, J.E. Rodríguez-Gil, S. Bonet, N. Prieto-Martínez, Aquaporins in the male reproductive tract and sperm: functional implications and cryobiology, *Reprod. Domest. Anim.* 52 (2017) 12–27, <https://doi.org/10.1111/rda.13082>.
- [12] R.N. Finn, J. Cerdá, Aquaporin evolution in fishes, *Front. Physiol. JUL* (2011), <https://doi.org/10.3389/fphys.2011.00044>.
- [13] R.N. Finn, J. Cerdá, C. Cerdá, *Evolution and Functional Diversity of Aquaporins, 2015*.
- [14] J. Cao, F. Shi, Comparative analysis of the aquaporin gene family in 12 fish species, *Animals* 9 (2019), <https://doi.org/10.3390/ani9050233>.
- [15] K. Ishibashi, Y. Morishita, Y. Tanaka, The evolutionary aspects of aquaporin family, *Adv. Exp. Med. Biol.* 969 (2017) 35–50, https://doi.org/10.1007/978-94-024-1057-0_2/COVER.
- [16] L.S. King, D. Kozono, P. Agre, From structure to disease: the evolving tale of aquaporin biology, *Nat. Rev. Mol. Cell Biol.* 5 (2004) 687–698, <https://doi.org/10.1038/nrm1469>.
- [17] M. Poveda, S. Hashimoto, Y. Enokiya, M. Matsuki-Fukushima, H. Sasaki, K. Sakurai, M. Shimono, *Expression and Localization of Aqua-glyceroporins AQP3 and AQP9 in Rat Oral Epithelia*, 2014.
- [18] S. Raina, G.M. Preston, W.B. Guggino, P. Agre, Molecular cloning and characterization of an aquaporin cDNA from salivary, lacrimal, and respiratory tissues, *J. Biol. Chem.* 270 (1995) 1908–1912, <https://doi.org/10.1074/jbc.270.4.1908>.
- [19] S.R. Harvey, C. O'Neale, K.L. Schey, V.H. Wysocki, Native mass spectrometry and surface induced dissociation provide insight into the post-translational modifications of tetrameric AQPO isolated from bovine eye lens, *Anal. Chem.* 94 (2022) 1515–1519, https://doi.org/10.1021/ACS.ANALCHEM.1C04322/ASSET/IMAGES/LARGE/AC1C04322_0003.JPG.
- [20] D. Yuan, W. Li, Y. Hua, G.J. King, F. Xu, L. Shi, Genome-wide identification and characterization of the aquaporin gene family and transcriptional responses to boron deficiency in brassica napus, *Front. Plant Sci.* 8 (2017), <https://doi.org/10.3389/fpls.2017.01336>.
- [21] S. Li, C. Li, W. Wang, *Molecular Aspects of Aquaporins*, in: *Vitam. Horm.*, Academic Press Inc., 2020, pp. 129–181, <https://doi.org/10.1016/bs.vh.2019.08.019>.
- [22] B. Nico, D. Ribatti, Aquaporins in tumor growth and angiogenesis, *Cancer Lett.* 294 (2010) 135–138, <https://doi.org/10.1016/j.canlet.2010.02.005>.
- [23] M. Hara-Chikuma, A.S. Verkman, Physiological roles of glycerol-transporting aquaporins: the aquaglyceroporins, *Cell. Mol. Life Sci.* 63 (2006) 1386–1392, <https://doi.org/10.1007/s00018-006-6028-4>.
- [24] K. Ishibashi, S. Kondo, S. Hara, Y. Morishita, The evolutionary aspects of aquaporin family, *Am. J. Physiol. - Regul. Integr. Comp. Physiol.* 300 (2011) 566–576, <https://doi.org/10.1152/ajpregu.90464.2008>.
- [25] C. Li, W. Wang, *Molecular Biology of Aquaporins*, in: *Adv. Exp. Med. Biol.*, Springer New York LLC, 2017, pp. 1–34, https://doi.org/10.1007/978-94-024-1057-0_1.
- [26] Y. Yang, H. Nishimura, Bird aquaporins: molecular machinery for urine concentration, *Biochim. Biophys. Acta - Biomembr.* 1863 (2021), <https://doi.org/10.1016/j.bbamem.2021.183688>.
- [27] M. Xiao, G. Hu, Involvement of aquaporin 4 in astrocyte function and neuropsychiatric disorders, *CNS Neurosci. Ther.* 20 (2014) 385, <https://doi.org/10.1111/CNS.12267>.
- [28] A. Mobasher, R. Barrett-Jolley, Aquaporin water channels in the mammary gland: from physiology to pathophysiology and neoplasia, *J. Mammary Gland Biol. Neoplasia* 19 (2014) 91–102, <https://doi.org/10.1007/s10911-013-9312-6>.
- [29] R.R. Geyer, R. Musa-Aziz, X. Qin, W.F. Boron, Relative CO₂/NH₃ selectivities of mammalian aquaporins 0–9, *Am. J. Physiol. - Cell Physiol.* 304 (2013), <https://doi.org/10.1152/ajpcell.00033.2013>.
- [30] A. Rojek, J. Praetorius, J. Frøkjær, S. Nielsen, R.A. Fenton, A current view of the mammalian aquaglyceroporins, *Annu. Rev. Physiol.* 70 (2008) 301–327, <https://doi.org/10.1146/annurev.physiol.70.113006.100452>.
- [31] T. Morinaga, M. Nakakoshi, A. Hirao, M. Imai, K. Ishibashi, Mouse aquaporin 10 gene (AQP10) is a pseudogene, *Biochem. Biophys. Res. Commun.* 294 (2002) 630–634, [https://doi.org/10.1016/S0006-291X\(02\)00536-3](https://doi.org/10.1016/S0006-291X(02)00536-3).
- [32] Y. Tanaka, Y. Morishita, K. Ishibashi, Aquaporin10 is a pseudogene in cattle and their relatives, *Biochem. Biophys. Reports.* 1 (2015) 16–21, <https://doi.org/10.1016/j.bbrep.2015.03.009>.
- [33] Z. Verdoucq, Aquaporins in plants, *Physiol. Rev.* 95 (2015) 1321–1358, <https://doi.org/10.1152/physrev.00008.2015-Aquaporins>.
- [34] A. Tanghe, P. Van Dijk, J.M. Thevelein, Why do microorganisms have aquaporins? *Trends Microbiol.* 14 (2006) 78–85, <https://doi.org/10.1016/J.TIM.2005.12.001>.
- [35] E.M. Campbell, B. Ball, S. Hoppler, A.S. Bowman, Invertebrate aquaporins: a review, *J. Comp. Physiol. B* 178 (2008) 935–955, <https://doi.org/10.1007/S00360-008-0288-2>.
- [36] F. Chauvigné, O. Yilmaz, A. Ferré, P.G. Fjeldal, R.N. Finn, J. Cerdá, The vertebrate Aqp14 water channel is a neuropeptide-regulated polytransporter, *Commun. Biol.* 2 (2019) 1–13, <https://doi.org/10.1038/s42003-019-0713-y>.
- [37] C. Cui, K.Q. Schoenfelt, K.M. Becker, L. Becker, Isolation of Polymorphonuclear Neutrophils and Monocytes From a Single Sample of Human Peripheral Blood, (n.d.), doi:<https://doi.org/10.1016/j.xpro.2021.100845>.
- [38] A. Vats, D. Gautam, J. Maharana, J. Singh Chera, S. Kumar, P.K. Rout, D. Werling, S. De, Poly I:C stimulation in-vitro as a marker for an antiviral response in different

- cell types generated from Buffalo (*Bubalus bubalis*), Mol. Immunol. 121 (2020) 136–143, <https://doi.org/10.1016/j.molimm.2020.03.004>.
- [39] M. Bonkobara, M. Hoshino, H. Yagihara, K. Tamura, M. Isotani, Y. Tanaka, T. Washizu, K. Arizumi, Identification and gene expression of bovine C-type lectin dectin-2, Vet. Immunol. Immunopathol. 110 (2006) 179–186, <https://doi.org/10.1016/J.VETIMM.2005.08.031>.
- [40] J. Sambrook, D.W. Russell, Purification of nucleic acids by extraction with phenol: chloroform, Cold Spring Harb. Protoc. 2006 (2006) pdb.prot4455, <https://doi.org/10.1101/PDB.PROT4455>.
- [41] A. Marchler-Bauer, S. Lu, J.B. Anderson, F. Chitsaz, M.K. Derbyshire, C. DeWeese-Scott, J.H. Fong, L.Y. Geer, R.C. Geer, N.R. Gonzales, M. Gwadz, D.I. Hurwitz, J. D. Jackson, Z. Ke, C.J. Lanczycki, F. Lu, G.H. Marchler, M. Mullokandov, M. V. Omelchenko, C.L. Robertson, J.S. Song, N. Thanki, R.A. Yamashita, D. Zhang, N. Zhang, C. Zheng, S.H. Bryant, CDD: a Conserved Domain Database for the functional annotation of proteins, Nucleic Acids Res. 39 (2011), <https://doi.org/10.1093/NAR/GKQ1189>.
- [42] I. Letunic, S. Khedkar, P. Bork, SMART: recent updates, new developments and status in 2020, Nucleic Acids Res. 49 (2021) D458–D460, <https://doi.org/10.1093/nar/gkaa937>.
- [43] S. Kumar, G. Stecher, M. Li, C. Knyaz, K. Tamura, MEGA X: molecular evolutionary genetics analysis across computing platforms, Mol. Biol. Evol. 35 (2018) 1547–1549, <https://doi.org/10.1093/MOLBEV/MSY096>.
- [44] A. Stamatakis, RAxML version 8: a tool for phylogenetic analysis and post-analysis of large phylogenies, Bioinformatics 30 (2014) 1312–1313, <https://doi.org/10.1093/BIOINFORMATICS/BTU033>.
- [45] A. Stamatakis, P. Hoover, J. Rougemont, A rapid bootstrap algorithm for the RAxML web servers, Syst. Biol. 57 (2008) 758–771, <https://doi.org/10.1080/10635150802429642>.
- [46] J. Zhang, R. Nielsen, Z. Yang, Evaluation of an improved branch-site likelihood method for detecting positive selection at the molecular level, Mol. Biol. Evol. 22 (2005) 2472–2479, <https://doi.org/10.1093/MOLBEV/MSI237>.
- [47] J.P. Bielawski, Z. Yang, Maximum likelihood methods for detecting adaptive protein evolution, Stat. Methods Mol. Evol. (2005) 103–124, https://doi.org/10.1007/0-387-27733-1_5.
- [48] W.H. Gharib, M. Robinson-Rechavi, The branch-site test of positive selection is surprisingly robust but lacks power under synonymous substitution saturation and variation in GC, Mol. Biol. Evol. 30 (2013) 1675–1686, <https://doi.org/10.1093/molbev/mst062>.
- [49] J. Zhang, R. Nielsen, Z. Yangà, Evaluation of an Improved Branch-site Likelihood Method for Detecting Positive Selection at the Molecular Level, 2015, <https://doi.org/10.1093/molbev/msi237>.
- [50] Z. Yang, PAML 4: phylogenetic analysis by maximum likelihood, Mol. Biol. Evol. 24 (2007) 1586–1591, <https://doi.org/10.1093/molbev/msm088>.
- [51] F. Gao, C. Chen, D.A. Arab, Z. Du, Y. He, S.Y.W. Ho, EasyCodeML: a visual tool for analysis of selection using CodeML, Ecol. Evol. 9 (2019) 3891–3898, <https://doi.org/10.1002/ee3.5015>.
- [52] Y. Benjamini, A.M. Krieger, D. Yekutieli, Adaptive linear step-up procedures that control the false discovery rate, Biometrika 93 (2006) 491–507, <https://doi.org/10.1093/BIOMET/93.3.491>.
- [53] G.M. Morris, H. Ruth, W. Lindstrom, M.F. Sanner, R.K. Belew, D.S. Goodsell, A. J. Olson, Software news and updates AutoDock4 and AutoDockTools4: automated docking with selective receptor flexibility, J. Comput. Chem. 30 (2009) 2785–2791, <https://doi.org/10.1002/jcc.21256>.
- [54] W.D.-C.N.P. Crystallogr, Pymol: An open-source molecular graphics tool, Citeseer (n.d.), <http://citeseerkse.ist.psu.edu/viewdoc/download?doi=10.1.1.231.5879&rep=rep1&type=pdf#page=44>, undefined 2002 (accessed May 16, 2022).
- [55] K.J. Livak, T.D. Schmittgen, Analysis of relative gene expression data using real-time quantitative PCR and the 2- $\Delta\Delta CT$ method, Methods 25 (2001) 402–408, <https://doi.org/10.1006/meth.2001.1262>.
- [56] H. Lorente-Martínez, A. Agorreta, M. Torres-Sánchez, D. San Mauro, Evidence of positive selection suggests possible role of aquaporins in the water-to-land transition of mudskippers, Org. Divers. Evol. 18 (2018) 499–514, <https://doi.org/10.1007/s13127-018-0382-6>.
- [57] R.N. Finn, F. Chauvigné, J.B. Hlidberg, C.P. Cutler, J. Cerdà, The lineage-specific evolution of aquaporin gene clusters facilitated tetrapod terrestrial adaptation, PLoS One 9 (2014), <https://doi.org/10.1371/journal.pone.0113686>.
- [58] B. Wu, E. Beitz, Aquaporins with selectivity for unconventional permeants, Cell. Mol. Life Sci. 64 (2007) 2413–2421, <https://doi.org/10.1007/S00018-007-7163-2/METRICS>.
- [59] S. Rajput, D. Gautam, A. Vats, C. Rana, M. Behera, M. Roshan, A. Ludri, S. De, Adaptive selection in the evolution of aquaglyceroporins in mammals, J. Mol. Evol. (2023), <https://doi.org/10.1007/S00239-023-10112-5>.
- [60] J.P. Tomkins, The human GULO pseudogene - evidence for evolutionary discontinuity and genetic entropy, Answers Res. J. 7 (2014) 91–101, <https://answeringgenesis.org/genetics/human-gulo-pseudogene-evidence-evolutionary-discontinuity-and-genetic-entropy/>.
- [61] L. Broccieri, E. Conway De Macario, A.J.L. Macario, Hsp70 genes in the human genome: conservation and differentiation patterns predict a wide array of overlapping and specialized functions, BMC Evol. Biol. 8 (2008) 1–20, <https://doi.org/10.1186/1471-2148-8-19>.
- [62] M.F. Flajnik, M. Kasahara, Comparative genomics of the MHC: glimpses into the evolution of the adaptive immune system, Immunity 15 (2001) 351–362, [https://doi.org/10.1016/S1074-7613\(01\)00198-4](https://doi.org/10.1016/S1074-7613(01)00198-4).
- [63] E. Kim, A. Goren, G. Ast, Alternative splicing: current perspectives, BioEssays 30 (2008) 38–47, <https://doi.org/10.1002/BIES.20692>.
- [64] R.D. Isokpehi, R.V. Rajnarayanan, C.D. Jeffries, T.O. Oyeleye, H.H.P. Cohly, Integrative sequence and tissue expression profiling of chicken and mammalian aquaporins, BMC Genomics 10 (2009) 1–12, <https://doi.org/10.1186/1471-2164-10-S2-S7>.
- [65] F. Staniscuaski, J.P. Paluzzi, R. Real-Guerra, C.R. Carlini, I. Orchard, Expression analysis and molecular characterization of aquaporins in rhodnius prolixus, J. Insect Physiol. 59 (2013) 1140–1150, <https://doi.org/10.1016/j.jinsphys.2013.08.013>.
- [66] Z. Wang, Y. Chen, C. Wang, N. Zhao, Z. Zhang, Z. Deng, Y. Cui, R. Wang, Y. Li, Aquaporins in Pacific white shrimp (*Litopenaeus vannamei*): molecular characterization, expression patterns, and transcriptome analysis in response to salinity stress, Front. Mar. Sci. 9 (2022), <https://doi.org/10.3389/fmars.2022.817868>.
- [67] H.H.P. Cohly, R. Isokpehi, R.V. Rajnarayanan, Compartmentalization of aquaporins in the human intestine, Int. J. Environ. Res. Public Health 5 (2008) 115–119, <https://doi.org/10.3390/ijerph502015>.
- [68] K. Kishida, I. Shimomura, H. Kondo, H. Kuriyama, Y. Makino, H. Nishizawa, N. Maeda, M. Matsuda, N. Ouchi, S. Kihara, Y. Kurachi, T. Funahashi, Y. Matsuzawa, Genomic structure and insulin-mediated repression of the aquaporin adipose (AQPop), adipose-specific glycerol channel, J. Biol. Chem. 276 (2001) 36251–36260, <https://doi.org/10.1074/JBC.M106040220>.
- [69] Y. Tutar, Pseudogenes, Comp. Funct. Genomics 2012 (2012) 6–9, <https://doi.org/10.1155/2012/424526>.
- [70] H. Kondo, I. Shimomura, K. Kishida, H. Kuriyama, Y. Makino, H. Nishizawa, M. Matsuda, N. Maeda, H. Nagaretani, S. Kihara, Y. Kurachi, T. Nakamura, T. Funahashi, Y. Matsuzawa, Human aquaporin adipose (AQPop) gene: Genomic structure, promoter analysis and functional mutation, Eur. J. Biochem. 269 (2002) 1814–1826, <https://doi.org/10.1046/J.1432-1033.2002.02821.X>.
- [71] O. Yilmaz, F. Chauvigné, A. Ferré, F. Nilsen, P.G. Fjelldal, J. Cerdà, R.N. Finn, Unravelling the complex duplication history of deuterostome glycerol transporters, Cells 9 (2020), <https://doi.org/10.3390/cells9071663>.
- [72] Y. Tanaka, Y. Morishita, K. Ishibashi, Aquaporin10 is a pseudogene in cattle and their relatives, Biochem. Biophys. Reports. 1 (2015) 16–21, <https://doi.org/10.1016/j.bbrep.2015.03.009>.
- [73] S.L.S. Pedro, J.M.P. Alves, A.S. Barreto, A.O. De Souza Lima, Evidence of positive selection of aquaporins genes from pontoporia blainvillei during the evolutionary process of cetaceans, PloS One 10 (2015) 1–11, <https://doi.org/10.1371/journal.pone.0134516>.
- [74] Y. Zang, J. Chen, H. Zhong, J. Ren, W. Zhao, Q. Man, S. Shang, X. Tang, Genome-wide analysis of the aquaporin gene family in reptiles, Int. J. Biol. Macromol. 126 (2019) 1093–1098, <https://doi.org/10.1016/j.ijbiomac.2019.01.007>.
- [75] N.J. Foot, S. Orgeig, S. Donnellan, T. Bertozzi, C.B. Daniels, Positive selection in the N-terminal extramembrane domain of lung surfactant protein C (SP-C) in marine mammals, J. Mol. Evol. 65 (2007) 12–22, <https://doi.org/10.1007/s00239-006-0083-1>.
- [76] S. Xu, Y. Yang, X. Zhou, J. Xu, K. Zhou, G. Yang, Adaptive evolution of the osmoregulation-related genes in cetaceans during secondary aquatic adaptation, BMC Evol. Biol. 13 (2013), <https://doi.org/10.1186/1471-2148-13-189>.
- [77] S.M. Ghoreishifar, S. Eriksson, A.M. Johansson, M. Khansefid, S. Moghaddaszadeh-Ahrabi, N. Parna, P. Davoudi, A. Javanmard, Signatures of selection reveal candidate genes involved in economic traits and cold acclimation in five Swedish cattle breeds, Genet. Sel. Evol. 52 (2020) 1–15, <https://doi.org/10.1186/s12711-020-00571-5>.
- [78] X. Xia, K. Qu, Y. Wang, M.H.S. Sinding, F. Wang, Q. Hanif, Z. Ahmed, J.A. Lenstra, J. Han, C. Lei, N. Chen, Global dispersal and adaptive evolution of domestic cattle: a genomic perspective, Stress Biol. 3 (2023), <https://doi.org/10.1007/s44154-023-00085-2>.
- [79] K. Liu, D. Kozono, Y. Kato, P. Agre, A. Hazama, M. Yasui, Conversion of aquaporin 6 from an anion channel to a water-selective channel by a single amino acid substitution, Proc. Natl. Acad. Sci. U. S. A. 102 (2005) 2192–2197, <https://doi.org/10.1073/PNAS.0409232102>.
- [80] D. Thomas, J. Gouranton, I. Pellerin, Switch from an Aquaporin to a Glycerol Channel by Two Amino Acids Substitution*, 1999, <https://doi.org/10.1074/jbc.274.11.6817>.
- [81] J. Yde, S.J. Keely, H.B. Moeller, Expression, regulation and function of Aquaporin-3 in colonic epithelial cells, Biochim. Biophys. Acta Biomembr. 1863 (2021) 183619, <https://doi.org/10.1016/j.bbamem.2021.183619>.
- [82] J.E. Hansen, L. Leslie, S. Swamy-mruthinti, The kinetics of thermal stress induced denaturation of Aquaporin 0, Biochem. Biophys. Res. Commun. 450 (2014) 1668–1672, <https://doi.org/10.1016/j.bbrc.2014.07.056>.
- [83] S. Swamy-Mruthinti, V. Srinivas, J.E. Hansen, C.M. Rao, Thermal stress induced aggregation of aquaporin 0 (AQPO) and protection by α -crystallin via its chaperone function, PloS One 8 (2013) e80404, <https://doi.org/10.1371/JOURNAL.PONE.0080404>.
- [84] Y. Shen, H. Li, J. Zhao, S. Tang, Y. Gu, X. Chen, Genomic and expression characterization of aquaporin genes from *Siniperca chuatsi*, Comp. Biochem. Physiol. Part D Genomics Proteomics 38 (2021) 100819, <https://doi.org/10.1016/J.CBD.2021.100819>.
- [85] D. Ramsköld, E.T. Wang, C.B. Burge, R. Sandberg, An abundance of ubiquitously expressed genes revealed by tissue transcriptome sequence data, PLoS Comput. Biol. 5 (2009) 1000598, <https://doi.org/10.1371/journal.pcbi.1000598>.
- [86] A. Mobasher, B.H. Kendall, J.E.J. Maxwell, A.V. Sawran, A.J. German, D. Marples, M.R. Luck, M.D. Royal, Cellular localization of aquaporins along the secretory pathway of the lactating bovine mammary gland: an immunohistochemical study, Acta Histochem. 113 (2011) 137–149, <https://doi.org/10.1016/j.acthis.2009.09.005>.

- [87] K. Michałek, M. Grabowska, Investigating cellular location of aquaporins in the bovine kidney. A new view on renal physiology in cattle, *Res. Vet. Sci.* 125 (2019) 162–169, <https://doi.org/10.1016/j.rvsc.2019.06.005>.
- [88] C. Zhong, A. Farrell, G.S. Stewart, Localization of aquaporin-3 proteins in the bovine rumen, *J. Dairy Sci.* 103 (2020) 2814–2820, <https://doi.org/10.3168/jds.2019-17735>.
- [89] K. Rump, M. Adamzik, Function of aquaporins in sepsis: a systematic review, *Cell Biosci.* 8 (2018) 1–7, <https://doi.org/10.1186/s13578-018-0211-9>.
- [90] C. Costa, R. Tortosa, A. Rodríguez, I. Ferrer, J.M. Torres, A. Bassols, M. Pumarola, Aquaporin 1 and aquaporin 4 overexpression in bovine spongiform encephalopathy in a transgenic murine model and in cattle field cases, *Brain Res.* 1175 (2007) 96–106, <https://doi.org/10.1016/j.brainres.2007.06.088>.
- [91] G. Chen, H. Song, Z. Yang, T. Du, Y. Zheng, Z. Lu, K. Zhang, D. Wei, AQP5 is a novel prognostic biomarker in pancreatic adenocarcinoma, *Front. Oncol.* 12 (2022) 1–15, <https://doi.org/10.3389/fonc.2022.890193>.
- [92] M. Yeste, R. Morató, J.E. Rodríguez-Gil, S. Bonet, N. Prieto-Martínez, Aquaporins in the male reproductive tract and sperm: functional implications and cryobiology, *Reprod. Domest. Anim.* 52 (2017) 12–27, <https://doi.org/10.1111/rda.13082>.
- [93] B.C. Schimming, C.A.E. Baumam, P.F.F. Pinheiro, R. de Matteis, R.F. Domeniconi, Aquaporin 9 is expressed in the epididymis of immature and mature pigs, *Reprod. Domest. Anim.* 52 (2017) 617–624, <https://doi.org/10.1111/rda.12957>.
- [94] R. Morató, N. Prieto-Martínez, R. Muñoz, C.O. Hidalgo, J.E. Rodríguez-Gil, S. Bonet, M. Yeste, Aquaporin 11 is related to cryotolerance and fertilising ability of frozen-thawed bull spermatozoa, *Reprod. Fertil. Dev.* 30 (2018) 1099–1108, <https://doi.org/10.1071/RD17340>.